University of Windsor
Scholarship at UWindsor

Electronic Theses and Dissertations | Theses, Dissertations, and Major Papers

8-22-1966

Kinetics of catalytic oxidation of methane application of initial rate technique for mechanism determination.

Om Parkash Ahuja
University of Windsor

Follow this and additional works at: https://scholar.uwindsor.ca/etd

Recommended Citation

Ahuja, Om Parkash, "Kinetics of catalytic oxidation of methane application of initial rate technique for mechanism determination." (1966). *Electronic Theses and Dissertations*. 6411.
https://scholar.uwindsor.ca/etd/6411

This online database contains the full-text of PhD dissertations and Masters' theses of University of Windsor students from 1954 forward. These documents are made available for personal study and research purposes only, in accordance with the Canadian Copyright Act and the Creative Commons license—CC BY-NC-ND (Attribution, Non-Commercial, No Derivative Works). Under this license, works must always be attributed to the copyright holder (original author), cannot be used for any commercial purposes, and may not be altered. Any other use would require the permission of the copyright holder. Students may inquire about withdrawing their dissertation and/or thesis from this database. For additional inquiries, please contact the repository administrator via email (scholarship@uwindsor.ca) or by telephone at 519-253-3000ext. 3208.

KINETICS OF CATALYTIC OXIDATION OF METHANE
APPLICATION OF INITIAL RATE TECHNIQUE
FOR MECHANISM DETERMINATION

A THESIS

Submitted to the Faculty of Graduate Studies through the Department of Chemical Engineering in Partial Fulfilment of the requirements for the degree of Master of Applied Science at University of Windsor

by
Om Parkash Ahuja

Windsor, Ontario, Canada
April, 1966

Reproduced with permission of the copyright owner. Further reproduction prohibited without permission.

UMI Number: EC52592

INFORMATION TO USERS

The quality of this reproduction is dependent upon the quality of the copy submitted. Broken or indistinct print, colored or poor quality illustrations and photographs, print bleed-through, substandard margins, and improper alignment can adversely affect reproduction.

In the unlikely event that the author did not send a complete manuscript and there are missing pages, these will be noted. Also, if unauthorized copyright material had to be removed, a note will indicate the deletion.

UMI®

UMI Microform EC52592
Copyright 2008 by ProQuest LLC.
All rights reserved. This microform edition is protected against unauthorized copying under Title 17, United States Code.

ProQuest LLC
789 E. Eisenhower Parkway
PO Box 1346
Ann Arbor, MI 48106-1346

Reproduced with permission of the copyright owner. Further reproduction prohibited without permission.

AAV 8980

Approved by:

147497

Reproduced with permission of the copyright owner. Further reproduction prohibited without permission.

ABSTRACT

A kinetic investigation on the oxidation of methane using a palladium catalyst was conducted. A differential bed reactor was used, and the conversions of methane were limited to about 10%. The small conversions facilitated the use of the initial rate approach to find the reaction mechanism. Plots of initial rate against total pressure were used to interpret the data qualitatively. Linearised rate equations were used to find the regression coefficients for various plausible mechanisms. The criteria of best fit to experimental data eliminated many improbable mechanisms.

Data on the variation of initial rate with feed composition were very helpful in arriving at a definite mechanism for the oxidation reaction. The experimental results indicated that the reaction rate was controlled by surface reaction in which the adsorbed oxygen and adsorbed methane react to produce adsorbed carbon dioxide and adsorbed water. The corresponding rate equation has the form:

$$r = \frac{C\left[P_{CH_4} P_{O_2}^2 - P_{H_2O}^2 P_{CO_2}/K\right]}{\left[1 + K_{CH_4} P_{CH_4} + K_{O_2} P_{O_2} + K_{CO_2} P_{CO_2} + K_{H_2O} P_{H_2O}\right]^3}$$

Reproduced with permission of the copyright owner. Further reproduction prohibited without permission.

ACKNOWLEDGEMENTS

The author wishes to express his sincere gratitude to Dr. G.P. Mathur for his able guidance, valuable suggestions and constructive criticism, to Dr. A.W. Gnyp for his guidance and direction, to Dr. S.J.W. Price, who provided his valuable time and guidance for operation of the gas chromatograph.

The financial assistance offered by National Research Council of Canada, in gratefully acknowledged.

Reproduced with permission of the copyright owner. Further reproduction prohibited without permission.

TABLE OF CONTENTS

	ABSTRACT	(i)
	ACKNOWLEDGEMENTS	(ii)
	TABLE OF CONTENTS	(iii)
	LIST OF TABLES	(v)
	LIST OF FIGURES	(vi)
CHAPTER		Page
I	INTRODUCTION - - - - - - - - - - - - - - - - - -	1
II	LITERATURE REVIEW - - - - - - - - - - - - - - - - - -	4
	A. Survey of Oxidation Catalysts for Exhaust Gases - - - - - -	4
	B. Kinetic Studies of Oxidation of Hydrocarbons - - - - - - -	5
	C. Important Considerations for Design of Catalytic Converter - -	7
III	THEORETICAL CONSIDERATIONS - - - - - - - - - -	10
IV	EXPERIMENTAL EQUIPMENT AND MATERIAL - - - - -	15
	A. Reactor, Preheater and Accessories - - - -	15
	B. Flow Measurement Devices - - - - - - - - - -	19
	C. Analytical Set-up - - - - - - - - - - - - - -	19
	D. Catalyst Choice - - - - - - - - - - - - - - -	19
	E. Selection of Gases - - - - - - - - - - - - - -	20
V	OPERATIONAL DETAILS AND RESULTS - - - - - - -	21
	A. Calibration Procedures - - - - - - - - - - -	21
	B. Operations Procedure - - - - - - - - - - - -	24
	C. Results - - - - - - - - - - - - - - - - - - -	25
VI	ANALYSIS OF RESULTS - - - - - - - - - - - - - -	29
VII	CONCLUSIONS - - - - - - - - - - - - - - - - - - -	59

Reproduced with permission of the copyright owner. Further reproduction prohibited without permission.

		Page
NOMENCLATURE		61
BIBLIOGRAPHY		63
APPENDIX I	Tables 6, 7, 8, 9, 10 and 11	65
APPENDIX II	Calibration Curves	72
APPENDIX III	Sample Calculation of Initial Rate from Experimental Data	81
APPENDIX IV	Sample Calculation for Heat and Mass Transfer Effects	84
APPENDIX V	Computer Programmes and Results	92
	VITA AUCTORIS	99

Reproduced with permission of the copyright owner. Further reproduction prohibited without permission.

LIST OF TABLES

Table		Page
1	Experimental Results of Oxidation Runs	27
2	Initial Rate Equations for Probable Mechanisms	32
3	Regression Coefficients for Linearised Rate Equations	39
4	Mechanistic Rate Equation Data	45
4a	Results of Present Investigation vs Mezaki's Investigation	51
5	Empirical Rate Equation Data	53
6	Composition of Auto Exhaust Gases under Different Operating Conditions - I	66
7	Composition of Auto Exhaust Gases under Different Operating Conditions - II	67
8	Composition of Auto Exhaust Gases under Different Operating Conditions - III	68
9	Correlation between Space Velocity and Conversion of Methane	69
10	The Analysis of C.P. Grade Methane	70
11	Operating Data for Chromatographic Analysis	71

Reproduced with permission of the copyright owner. Further reproduction prohibited without permission.

LIST OF FIGURES

Figure		Page
1	Schematic Diagram of Experimental Equipment	16
2	Sectional View of Reactor tube and Differential Bed	17
3	Initial Rate of Reaction Vs Total Pressure 300°C	34
4	Initial Rate of Reaction Vs Total Pressure 320°C	35
5	Initial Rate of Reaction Vs Total Pressure 340°C	36
6	Initial Rate of Reaction Vs Feed Composition 300°C, 1.817 Atm.	41
7	Initial Rate of Reaction Vs Feed Composition 320°C, 1.817 Atm.	42
8	Initial Rate of Reaction Vs Feed Composition 340°C, 1.817 Atm.	43
9	Initial Rate of Reaction from Mechanistic Equation 300°C	48
10	Initial Rate of Reaction from Mechanistic Equation 320°C	49
11	Initial Rate of Reaction from Mechanistic Equation 340°C	50
12	Initial Rate of Reaction from Empirical Equation 300°C	56
13	Initial Rate of Reaction from Empirical Equation 320°C	57
14	Initial Rate of Reaction from Empirical Equation 340°C	58
15	Calibration Curves for Oxygen Rotameter	73

Reproduced with permission of the copyright owner. Further reproduction prohibited without permission.

LIST OF FIGURES (Cont'd)

Figure		Page
16	Calibration Curves for Methane Rotameter	74
17	Arrangement of Columns for 6-port Detector	75
18	Chromatographic Calibration for Carbon Dioxide	76
19	Chromatographic Calibration for Oxygen	77
20	Chromatographic Calibration for Nitrogen	78
21	Chromatographic Calibration for Methane	79
22	Chromatographic Calibration for Carbon Monoxide	80

Reproduced with permission of the copyright owner. Further reproduction prohibited without permission.

CHAPTER I

INTRODUCTION

Air pollution, in general, is a direct result of smoke, dust or fumes from a variety of sources. Processes like combustion, roasting, mining and quarying contribute greatly to air pollution.

The objectionable components from incomplete combustion of fuels in industry and automobiles are the hydrocarbons and oxides of nitrogen. Hydrocarbons and nitrogen oxides are present in such small concentrations that they probably have no direct effect on health. But, as reported by Yocom[1], the hydrocarbons react photochemically with nitrogen oxides to produce unstable peroxides which act as a nuclei in smog production. In major industrial cities, high concentrations of carbon monoxide, coming from combustion processes and automobiles, can cause toxic effect on humans.

At present the world's use of fuels is rising rapidly because of industrialisation and development. As a result the pollution hazard is growing. Reduction of smog forming components and carbon monoxide in tail gases would be a necessary step towards reducing air pollution.

Many devices[2] have been advanced so far for the prevention of these undesirable components in tail gases of automobiles. The following devices have been examined critically from a commercial point of view:

Reproduced with permission of the copyright owner. Further reproduction prohibited without permission.

1. After burners
2. Liquid washing devices
3. Adsorption units
4. Catalytic converters

The major problem in the design of after burners is maintenance of a flame which will allow auto-ignition of hydrocarbons under all conditions. Liquid washing devices and adsorption with porous solids have not been very successful so far, because of the unwieldy size of such devices. Catalytic conversion is a promising alternative to other devices.

Extensive investigations on catalytic converters for carbon monoxide and hydrocarbons, were made by Lamb and co-workers[3] towards the end of World War I. The investigations of Lamb and co-workers and of Yant and Hawk[4] showed that the catalysts effective for carbon monoxide oxidation are also effective for hydrocarbons oxidation. Recently reported laboratory evaluations of catalysts for the automotive exhausts by Cannon and Welling[5] confirm the earlier results.

Table 6, 7 and 8[6] in Appendix 1 show typical compositions of automotive exhaust gases under different operating conditions. These tables show that methane constitutes 25 to 40% of the total hydrocarbons in tail gases. Furthermore, Anderson and co-workers[7] have reported that, in the light hydrocarbons family, methane is the most difficult gas to oxidise.

The data obtained from the catalytic oxidation of methane should be helpful in the design of a suitable catalytic reactor for automobile exhaust control. In addition to this, a kinetic investigation of the methane oxidation should be very interesting from a scientific point of view.

Reproduced with permission of the copyright owner. Further reproduction prohibited without permission.

In the present investigation the objective was to establish the mechanism of catalytic oxidation of methane by using an initial rate approach. Obviously, the initial rate technique limited to low conversion experiments, does not provide data for design of catalytic converters for auto exhausts. Experiments at nearly complete conversion would be necessary to provide such information. However, integral rate data are difficult to evaluate from a mechanistic point of view.

For a study of a catalytic reaction, a two step process is recommended

(i) Initial rate analysis to establish the mechanistic equation.
(ii) High conversion study to fit the mechanistic equation in the desired conversion range.

The assumption that is inherent in the above scheme is that the adsorption characteristics of the components do not change over the range of conversion. This is considered a reasonable assumption for most catalytic reactions. The equilibrium quantities being function of temperature only, do not change with composition.

This investigation is concerned with the first stage of the scheme discussed above. Data at low conversion and varying pressure would be employed to establish the mechanistic equation. The rate equation obtained by initial rate approach, after addition of the proper product terms should be applicable for high conversion range.

Reproduced with permission of the copyright owner. Further reproduction prohibited without permission.

CHAPTER II

LITERATURE REVIEW

A. Survey of Oxidation Catalysts for Exhaust Gases

Many investigations[8] have been reported on the partial oxidation of hydrocarbons to valuable organic substances as acids, aldehydes, alcohols, esters and ketones. In addition to this, a large amount of work has been done on the catalytic oxidation of exhaust gases and individual hydrocarbon constituents.

As early as 1825, the effect of platinum on the combustion of methane at 290°C was investigated by Henry[9]. Yant and Hawk[4] found that platinum had a catalytic effect at temperatures between 150 to 300°C for approximately 4% methane in air. Conversion was less than 10% in this temperature range.

The catalytic activity of copper oxide for methane oxidation has been studied by Campbell[10], Wheeler[11] and Araki[13]. According to them, copper oxide has a catalytic activity at rather elevated temperatures, in the range of 400 - 700°C.

Yant and Hawk[4], Thompson [14], and Anderson and co-workers[7] found oxides of Ni, Cr, Mn, V and Co quite effective for methane oxidation. In particular, Co_3O_4 gave promising results with respect to conversion and catalyst life. According to recent experiments of Kazarnovskya and Dykhno[15], the most effective catalyst for oxidation of methane is manganic ore enriched with silver. The complete combustion of 0.10 - 0.15% methane in oxygen was observed at 300°C. The detailed description of this catalyst is not given.

Reproduced with permission of the copyright owner. Further reproduction prohibited without permission.

Towards the end of World War I, a commercial material called Hopcalite was discovered for carbon monoxide gas masks. Hopcalite is a registered trade name with the Mine Safety Appliance Company, and is really a mixture of compounds which indlude, among others, manganese dioxide and cuprous oxide. After extensive investigations, Lamb and co-workers[3] found that the mixture of oxides of copper, manganese, silver and cobalt was most effective for oxidation of carbon monoxide. Yant and Hawk[4] have reported that commercial Hopcalite could oxidise 4% methane in air to carbon dioxide and water with 10 - 60% conversion over the temperature range 200 - 350°C. This catalyst is quite effective for dry gas, but poisoned very rapidly in presence of water vapour. It also loses activity on prolonged heating at temperatures above 250°C, due to sintering.

Anderson and co-workers[7] have concluded that the catalytic activity of metals and their oxides, decreases in the following order: Pd, Pt, Cr, Mn, Cu, Ce, Co, Fe, Ni, and Ag. This order of effectiveness was the same as previously reported by Cohn and Haley[16].

B. Kinetic Studies on the Oxidation of Hydrocarbons

Anderson and co-workers[7] did a kinetic study on the oxidation of methane. The catalyst bed was 7 to 7.5 cc. deep with a cross section of 2.435 sq. cm., methane concentration was 1% and air flow 2 liters/min. at room temperature. Thirty kinds of catalysts were tested over the temperature range 450 - 800°K, using a constant value of space velocity. The experimental data were approximated by an empirical equation with respect to methane concentration.

Reproduced with permission of the copyright owner. Further reproduction prohibited without permission.

Rosenbaum[17] worked on the oxidation of very dilute methane (51 ppm in air) at 1075°F by using the pelletized catalyst supplied by Engelhard Industries. The relationship between space velocity and conversion is given in Table 9 in Appendix I. The volume of catalyst used was 0.0005 cu. ft. No details were given for the size and composition of the catalyst.

Mezaki[18] used vanadia, cobalt, copper-chromite, chrome alumina, hopcalite and palladium catalysts for methane oxidation. He found palladium to be the most effective catalyst from the stand point of ignition temperature, stability, freedom from side reactions, and good conversion. However, palladium is not necessarily free from objectionable features. It has a reported tendency of poisoning by lead compounds.

Mezaki studied the catalytic oxidation of methane using 0.5% palladium on alumina catalyst. Methane concentrations in feed were 1 to 2%. The reaction temperature was varied between 320 to 380°C and the pressure was kept atmospheric. The feed in addition to reactants contained reaction products as well. In this connection, Mezaki has correctly pointed out that when the feed to reactor contains the reaction products, one cannot use the initial rate - total pressure correlation to screen the postulated mechanisms.

In an initial survey, Mezaki[19] used 84 models in which adsorption of reactants or desorption of products was the postulated rate-controlling step. The linearised models were fitted to the experimental rate-data by least square technique, but this fitting resulted in two or more negative constants. This led to the rejection of these models.

Reproduced with permission of the copyright owner. Further reproduction prohibited without permission.

Then, assuming that surface reaction is the rate controlling step, Mezaki used integral kinetic equations for fitting the experimental data to postulated models. He eventually concluded that the controlling step in the oxidation of methane is surface reaction between adsorbed oxygen and gaseous methane to give adsorbed carbon dioxide and water. There is no apriori reason to suspect that in a catalytic reaction, at different temperatures, the same step is rate controlling. Recent applications of the initial rate technique have established that for the same catalytic reaction at different temperatures, different steps could be rate controlling. Thaller and Thodos[20] and Mathur[21] have reported changes in controlling step at different temperatures for two quite different types of catalytic reactions. In view of this, Mezaki's treatment of kinetic data appears to be somewhat empirical.

C. Important Considerations in the design of a Catalytic Converter

Many factors have to be considered for the design of a catalytic converter for auto exhausts. Different makes and life of automobiles, fuels and wide range of operating conditions lead to great variation in physical and chemical properties of exhaust gases. A brief review of the current situation follows.

(i) Exhaust Gas Temperature

Exhaust gas temperatures are changed by operating conditions. Temperatures from 150 to 1500°F have been observed depending on engine operation and location of measurement in tail gas pipe. Therefore, it is essential to determine the lowest temperature at which the

Reproduced with permission of the copyright owner. Further reproduction prohibited without permission.

catalytic conversion starts and highest working temperature of catalyst.

(ii) Exhaust Gas Flow Rate

From measured air intakes of passenger cars, computed exhaust volumes, at 1 Atm. and 70°F, range from 6 to 10 cfm. at idle, to 50 cfm. at 50 mph. The flow rate at accelration might reach 250 cfm.

(iii) Exhaust Gas Composition

Hydrocarbons, hydrogen and carbon monoxide are the major combustible components in the exhaust gases. The concentrations of these components vary greatly depending on operating conditions and air-fuel ratio. Tables 6, 7 and 8[6] in Appendix I show some typical compositions of automobile exhaust gases under different operating conditions.

If automobiles were running at fairly constant rates, the kinetics of exhaust gas oxidation could be solved for a steady state condition. When an automobile starts to run, the oxidation process gives a complicated unsteady state problem. Generally, an automobile starts in a residential area, goes through more.populated zones at variable engine conditions, and runs through sparsely populated areas at rather constant conditions. When the engine starts, it stays at a rather low temperature and the exhaust contains a large amount of carbon monoxide and hydrocarbons. Therefore, the oxidation catalyst needs to be specially active at low temperature.

Reproduced with permission of the copyright owner. Further reproduction prohibited without permission.

It should also have good conversion, good life, and inertness to lead compounts.

The pressure drop through the catalytic converter should be low to reduce power cost for compression of gases. The converter should also be compact in construction.

Reproduced with permission of the copyright owner. Further reproduction prohibited without permission.

CHAPTER III

THEORETICAL CONSIDERATIONS

In a solid catalyzed reaction the physical steps are the transfer of the fluid reactants upto the catalyst surface, diffusion of reactants into the interior of the pellet, diffusion of products back to the surface and transfer of products from the exterior surface to the main stream. To simplify the kinetic interpretation of the experimental data, these physical steps have to be minimised.

The chemical steps involve activated adsorption of reactants with or without dissociation, surface reaction on active sites and activated desorption of products. From an absolute theory point of view, the adsorption process is a bimolecular reaction involving a molecule or an atom from the gas phase and an active point on the catalyst surface.

In order to determine the mechanism of a catalytic reaction on the basis of the Hougen Model[21], various possible reaction schemes are investigated. The acceptability criteria for any rate equation is that all equilibrium constants have to be positive.

As an illustration, consider a scheme in which the surface reaction is between an adsorbed methane molecule and two oxygen molecules dissociated and adsorbed on dual sites. The rate equations for adsorption, surface reaction and desorption steps are deduced from the treatment given by Hougen[21]

Reproduced with permission of the copyright owner. Further reproduction prohibited without permission.

ADSORPTION STEPS

(i) Adsorption of oxygen:-

$$2\ O_2 + 2\ l_2 \rightleftharpoons 2\ O_2l_2 \qquad (1)$$

$$2\ O_2l_2 + 4\ l \rightleftharpoons 4\ Ol + 2\ l_2 \qquad (2)$$

Eq. (1) is rate controlling and equilibrium maintained in (2), net rate of adsorption of oxygen

$$R\ ads. = k_{o_2}\ a^2_{O_2}\ C^2_{l_2} - k'O_2\ \frac{\left[C_{Ol}\right]^4 \left[C_{l2}\right]^2}{K'o_2\ \left[C_l\right]^4} \qquad - (3)$$

(ii) Adsorption of methane:-

$$CH_4 + l \rightleftharpoons CH_4l \qquad (4)$$

net rate of adsorption of methane

$$r = k_{CH_4}\ a_{CH_4}\ C_l - k'_{CH_4}\ C_{CH_4l} \qquad (5)$$

SURFACE REACTION

Surface reaction between four adsorbed oxygen atoms and adsorbed methane molecule to give activated complex involving one carbon dioxide molecule and two water molecules and two active centres

$$4\ Ol + CH_4l \rightleftharpoons CO_2l + 2\ H_2Ol + 2\ l \qquad - (6)$$

net rate of surface reaction

$$R\ s.r. = \frac{s(s-l)\ ks.r.}{L^2} \left[C_{CH_4l}\ C^4_{Ol} - \frac{C_{CO_2l}\ C^2_{H_2Ol}\ C^2_l}{K's.r.} \right] \qquad (7)$$

Reproduced with permission of the copyright owner. Further reproduction prohibited without permission.

DESORPTION STEPS

(i) Desorption of Carbon dioxide

$$CO_2 l \rightleftharpoons CO_2 + l \qquad (8)$$

net rate of desorption of CO_2

$$r_{des.} = k'_{co_2} \; C_{co_2 l} - k_{co_2} \; a_{co_2} \; C_l \qquad (9)$$

(ii) Desorption of water

$$2H_2Ol \rightleftharpoons 2H_2O + 2\,l \qquad (10)$$

net rate of desorption of H_2O

$$r_{des.} = k'_{H_2O} \; C^2_{H_2Ol} - k_{H_2O} \; a^2_{H_2O} \; C^2_l \qquad (11)$$

If the adsorption of oxygen is rate controlling step and the adsorption of methane, the surface reaction, the desorption of CO_2 and H_2O are equilibrium steps. The rate of reaction would be

$$r = k_{O_2} \left(\frac{s}{2L}\right)^2 C^4_l \left[a^2_{O_2} - \frac{1}{K} \frac{a_{CO_2} \; a^2_{H_2O}}{a_{CH_4}} \right] \qquad (12)$$

C_l, total concentrations of vacant active centres, is given by

$$C_l = L - C_{CH_4 l} + C_{CO_2 l} + C_{H_2Ol} + C_{Ol} \qquad (13)$$

$$\text{or, } C_l = \frac{L}{\left[1 + K_{CH_4} a_{CH_4} + K_{CO_2} a_{CO_2} + K_{H_2O} a_{H_2O} + 4\sqrt{\frac{K_{O_2}}{K} \frac{a_{CO_2} \; a^2_{H_2O}}{a_{CH_4}}} \right]} \qquad (14)$$

Reproduced with permission of the copyright owner. Further reproduction prohibited without permission.

from (12) and (14)

$$r = \frac{ko_2\, s^2 L^2 \left[a^2_{O_2} - \frac{1}{K} \frac{a_{CO_2}\, a^2_{H_2O}}{a_{CH_4}} \right]}{4 \left[1 + K_{CH_4} a_{CH_4} + K_{CO_2} a_{CO_2} + K_{H_2O} a_{H_2O} + 4\sqrt{\frac{K_{O_2}}{K} \frac{a_{CO_2}\, a^2_{H_2O}}{a_{CH_4}}} \right]^4} \quad - (15)$$

If product concentrations are very small as compared to reactant concentrations, the rate of reaction can be written, as,

$$r = K \left[a^2_{o_2} \right] \Big/ \left[1 + K_{CH_4}\, a_{CH_4} \right]^4 \quad - (16)$$

For a constant ratio of methane to oxygen, and assuming ideal gas law condition, equation (16) can be written in terms of total pressure, π, as follows

$$ro = a\,\pi^2 \Big/ \left[1 + b\,\pi \right]^4 \quad - (17)$$

The simplicity and directness of the initial rate equation (17), as compared to the complete rate expression, equation (15), is obvious.

Yang and Hougen[22] pointed out that initial rate analysis is one of the best techniques to establish the mechanism of a catalytic reaction. They have discussed in detail the type of results that are to be anticipated when the initial rates are plotted against total pressure and feed composition.

Reproduced with permission of the copyright owner. Further reproduction prohibited without permission.

By systematic and independent variations in total pressure and feed composition, the plots of initial rates against total pressure and feed composition are obtained. Through an interpretation of these plots, it is possible to establish the rate controlling step or steps of the catalytic reaction with assurance. Moreover, initial rate approach does not assume that the same controlling step or steps are operative at all temperatures.

As pointed out in the introduction the initial rate equations are not complete rate equations for a catalytic reaction. The initial rate approach nevertheless provides for a much more direct determination of the mechanism of a catalytic reaction.

In this investigation the objective is to establish the mechanism of methane oxidation at different temperatures. The overwhelming advantages of the initial rate technique, as apposed to the conventional approaches, recommended for this investigation.

Reproduced with permission of the copyright owner. Further reproduction prohibited without permission.

CHAPTER IV

EXPERIMENTAL EQUIPMENT AND MATERIALS

The reaction rate data for the oxidation of methane was obtained using a differential bed reactor confined in a cylinderical tube. A schematic diagram of the set up is shown in Figure 1. The details of the equipment and materials used are given below:-

(A) Reactor, Preheater and Accessories

The reactor tube and the differential bed are shown in Figure 2. The reactor tube was made of 1½ inch I.D., schedule 40, 304 stainless steel tubing. The ends of the tube were fitted with 300 psig. welding neck flanges and matching blind flanges. Copper gaskets of 1/8 inch thickness were used for leakproof closure of the tube. Thermowells were welded to top and bottom flanges. To facilitate insertion of ¼" berl saddles, 3/8" O.D.S.S. tube was also welded to top and bottom flanges.

The differential bed consisted of a 1 3/8" O.D., 1/8" thick, 5 1/2" long S.S. cartridge. Its ends were closed by screens and washers. The screens fitted snugly with the inside of the reactor tube with little clearance. Catalyst mixed with ceramic berl saddles was charged into the cartridge. This minimised the non-uniformity of bed and channeling effects. The catalyst bed occupied the space between the ends of the thermowells, rest of reactor space was packed with 1/4" ceramic berl saddles.

Reproduced with permission of the copyright owner. Further reproduction prohibited without permission.

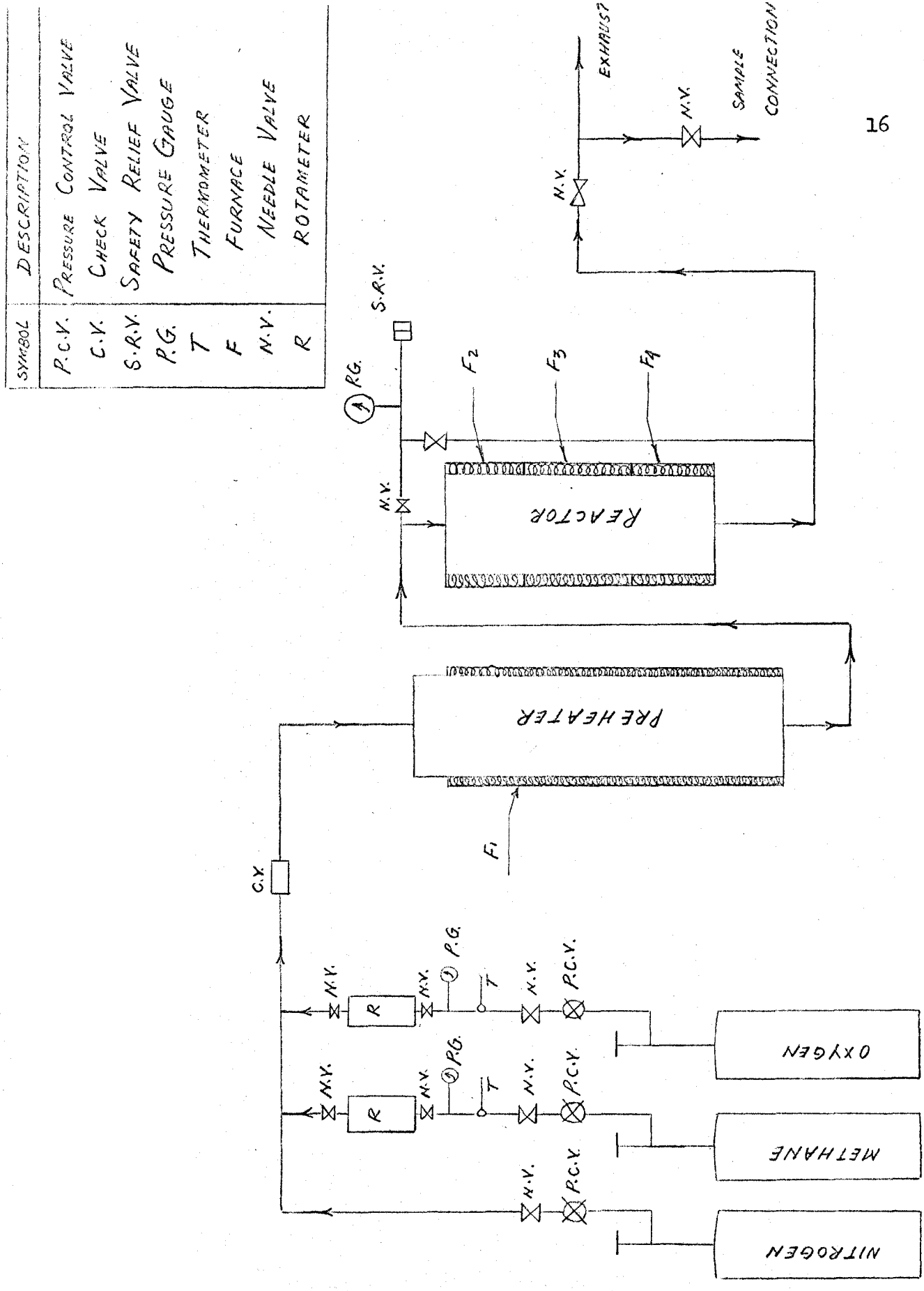

FIG. 1 SCHEMATIC DIAGRAM OF EXPERIMENTAL EQUIPMENT

Reproduced with permission of the copyright owner. Further reproduction prohibited without permission.

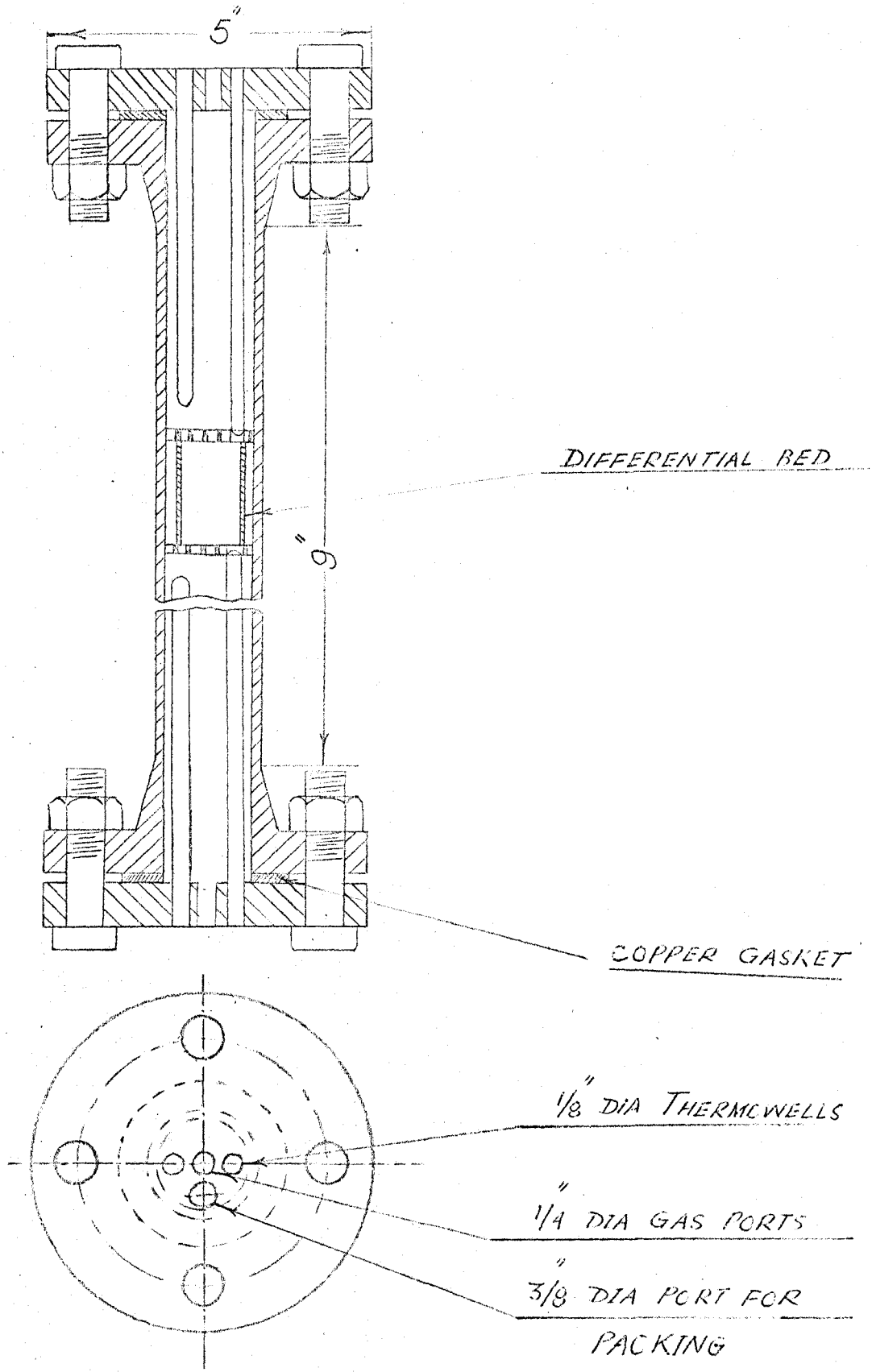

FIG. 2 SECTIONAL VIEW OF REACTOR TUBE AND DIFFERENTIAL BED

Reproduced with permission of the copyright owner. Further reproduction prohibited without permission.

The preheater construction was basically identical to that of the reactor. A minor difference was that reactor tube was 3 inches shorter than the preheater tube. The preheater was packed with 1/4" ceramic berl saddles.

The tubing connecting the gas cylinders to preheater was 1/4" O.D. Copper. From preheater exit to sampling connection, the tubing was 1/4" O.D. S.S. Standard screwed swagelok fittings were used for all connections.

The preheater was heated by 12" long, 1400 watts cylinderical heating units. The reactor had three independently controlled heating sections of lengths 3 1/2", 5" and 3 1/2" rated at 700, 1160 and 700 watts respectively. The furnaces were insulated with refractory fibre felt supplied by Johns Manville. To prevent condensation of water vapours in the system, the tubing from preheater exit to sampling connection was heated with electric heating tape.

Chromel-alumel thermocouples in 1/16" O.D. stainless steel sheaths were used for temperature measurement.

A pressure gauge of range 0-400 psig. with valve connections at the inlet and the outlet of the reactor, was used to measure the operating pressure of the system. A spring loaded pressure relief valve set at 500 pounds, was used as the safety device.

Reproduced with permission of the copyright owner. Further reproduction prohibited without permission.

(B) Flow Measurement Devices

Rotameters were used to measure the flow rates of oxygen and methane. These were equipped with dual floats, one of pyrex, the other of stainless steel. The maximum flow ranges with the two floats were 4.4 and 8.8 SCFH of air. The rotameters for oxygen and methane were identical in all respects. These were supplied by Matheson Co.

(C) Analytical Equipment

The analytical equipment for reactants and products was a gas chromatograph. It was a 5000 series selecta system model supplied by Barber Colman Ltd. It had dual column bath and six port thermal conductivity detector. The arrangement of the columns connected to the six ports is given in Figure 17 of Appendix II. The first column was a 1/4" O.D.; 1 ft. silica gel type followed by 1/4" O.D. 7 ft. molecular sieve column. The second column was 1/8" O.D.; 15 ft. carbowax 1500.

Other major parts of the chromatograph were carrier gas supply regulators, injector bath, column bath, detector filaments current supply and the recorder. All syringes were gas tight.

(D) The catalyst, 0.5% palladium on alumina supplied by Engelhard Industries Inc., had the following physical properties:-

Bulk density	56 pounds per cu. ft.
Surface area	120 square metres per gram.
Size	1/8" x 1/8" cylinderical pellets

Reproduced with permission of the copyright owner. Further reproduction prohibited without permission.

(E) Selection of Gases

(i) Oxygen gas was supplied by Liquid Carbonic Corporation and was of 99.9% purity.

(ii) Methane gas was of chemically pure grade supplied by Matheson Co. It was of minimum 99% purity. The typical average composition of the gas in given in Table 10, Appendix I.

(iii) Nitrogen and carbon dioxide used for calibration were of 99.9% purity and supplied by Liquid Carbonic Corporation.

(iv) Carbon monoxide used for calibration was of C.P. grade supplied by Matheson Co. It was of minimum 99.5% purity.

(v) The helium gas used as carrier in the chromatograph was of 99.99% purity. It was supplied by Liquid Carbonic Corporation. An alumina packed filter was used in the helium line to prevent, any trace of water vapour in the helium gas from entering the system.

Reproduced with permission of the copyright owner. Further reproduction prohibited without permission.

CHAPTER V

OPERATIONAL DETAILS AND RESULTS

The operational procedure for conduction of kinetic runs is summarised in this chapter.

(A) Calibration Procedure

(i) Calibration of Rotameters

For rotameters operating under a constant pressure difference but with a constriction of variable area, the mass flow rate is related to the scale reading by the following expression[23]

$$W = C_r A_o \left[\frac{2 g \rho (\rho_f - \rho)}{A_f} \right]^{1/2} \qquad (18)$$

Since the float density is normally an order of magnitude larger than the density of the fluid whose flow is being measured, equation (18) can be approximated to

$$\frac{W}{\sqrt{\rho}} = C_r A_o \qquad (19)$$

The coefficient of discharge Cr is sensitive to the viscosity and to the flow lines through the constriction. For high flow rates, Cr tends to assume a constant value, and for this reason it is convenient to calibrate the flow meters according to the procedure suggested by equation (19).

Reproduced with permission of the copyright owner. Further reproduction prohibited without permission.

The calibration of methane and oxygen rotameters was done by measuring actual flow rates with a precision wet-test meter. The upstream pressures and temperatures of the gases were measured by pressure gauges and thermometers installed in the lines before the rotameters inlet. Since neither of the gases is soluble in water, the presaturator of the wet test meter was filled with distilled water. The calibration curves for the rotameters over the complete range of investigation are given by Figures 15 and 16 in Appendix II

(ii) Calibration of Thermocouples

The chromel-alumel thermocouples used to measure temperatures were calibrated against the boiling point of distilled water and the melting points of chemically pure tin and zinc. The observed temperatures were extremely close to standard temperatures. Therefore, the error involved in measurement of experimental temperatures, is negligible.

(iii) Calibration of Chromatograph

(a) Principle

The carrier gas is introduced into the system at a specified flow rate. The column, injector and detector baths are heated to the required isothermal temperatures. These temperatures are chosen to prevent condensation of any component at any stage of the process. Another operational consideration is that separation of different components should be explicit. A sample mixture is then injected into the

Reproduced with permission of the copyright owner. Further reproduction prohibited without permission.

injector part. As the sample is carried through the columns, the components are separated according to their respective solubilities in the column charge. The components having little affinity for the column material pass through the column rapidly, while those with greater affinities are retained in the column for longer periods.

As each component emerges from the column, it is driven into the sensing side of the detector located immediately after the column exit. The other side of the detector which is the reference side is upstream of the sample injection block and is filled with carrier gas prior to the point at which the sample is injected. Thermistors in each chamber of the detector are connected to a balanced bridge circuit and are cooled by the gases to which they are exposed. When a component enters the sensing chamber, the thermistor bridge circuit is unbalanced and generates a signal. The signal is proportional to the difference in thermal conductivities of the carrier gas and the component. The signal drives a recorder pen to produce, in graphic form, a quantitative and qualitative description of the component.

(B) Calibration

Due to large number of components to be analyzed, the silica gel column, followed by molecular sieve column, were found to give explicit separation of all the desired components. The silica gel column gave combined peak and peak for carbon dioxide.

Reproduced with permission of the copyright owner. Further reproduction prohibited without permission.

The molecular sieve column gave separation for oxygen, nitrogen, methane and carbon monoxide.

The operating conditions for the analytical set-up are given by Table 11, in Appendix I.

The concentration of any component is directly proportional to the peak area. However, in this case, a measurement of peak height gave a reasonably accurate proportionality to component concentration. This relation was valid for pure components as well as for the mixtures used. The calibration curves for different components are given by figures 18 to 22, in Appendix II. The concentration of water was found by difference. Absence of alcohol and aldehydes was established during the trial runs of methane oxidation, thus calibrations for these components were not done.

(B) Operational Procedure

The preheater and reactor furnaces were switched on and variacs adjusted to heat the system to the desired temperature. Oxygen gas was fed through the rotameter, with the feed rate and reactor exit valve being adjusted for the desired working pressure. After the temperatures had stabilised, methane gas was slowly fed to the system through the rotameter. The flow-rates of oxygen and methane, the reactor exit valve and the variacs were adjusted for desired working pressure and isothermal temperature of the differential bed.

The reaction was allowed to proceed for about one hour, at the desired conditions, before the first sample was taken for analysis. Three samples were taken for each run. The average

Reproduced with permission of the copyright owner. Further reproduction prohibited without permission.

of the three readings was used to calculate the product composition. It took about fifteen minutes for analysis of each product sample. Therefore, each sample was withdrawn at an interval of fifteen to twenty minutes after the attainment of equilibrium conditions.

Preliminary runs confirmed Mezaki's [18] observations that the catalyst achieved uniform activity after twenty hours of service. Therefore, for each series of runs, the catalyst was first allowed to attain uniform activity.

Prior to the start of the runs, with the catalyst, blank runs were made with different oxygen methane ratios within the range of operating temperatures and pressures. These blank runs confirmed that no parts of the equipment contributed to the conversion.

(C) Results

Following the procedure outlined above, two series of runs were made. For both series the catalyst charge was 0.498 gm. One series of runs was with about 6% to 30% methane, at about 1.8 atmospheres total pressure and at temperatures of 300, 320 and 340°C. The second series of runs was made at almost constant feed composition of about 6.5% methane. The total pressure was varied from 1.8 to 9.7 atmospheres. The runs were at isothermal temperatures of 300, 320 and 340°C.

147497

UNIVERSITY OF WINDSOR LIBRARY

Reproduced with permission of the copyright owner. Further reproduction prohibited without permission.

The percentage of products was 0.4 to 1.2%, and conversions were 3.69 to 9.10%. For such small conversions, it is accurate enough to consider the reaction to be differential. Initial rates of reaction were computed from the expression

$$ro = \frac{X_{AO}}{W / F_{AO}} \qquad (20)$$

The method of computation of initial rate from experimental data, is given in Appendix III. The results of the experimental runs are given by Table 1.

Reproduced with permission of the copyright owner. Further reproduction prohibited without permission.

Reproduced with permission of the copyright owner. Further reproduction prohibited without permission.

Table - 1

Experimental Results of Oxidation Runs

Run No.	Temperature °C	Total Pressure Atm.	Flow Rate lb-moles/hr.		Conversion %	Rate of Reaction
			Methane	Oxygen	$\frac{\text{lb-moles } CH_4 \text{ converted}}{\text{lb-moles } CH_4 \text{ in feed}} \times 100$	$\frac{\text{lb-moles } CH_4 \text{ converted}}{\text{(hr.)(lb. of catalyst)}}$
I - 1	300	1.817	0.00474	0.0664	8.66	0.373
I - 2	320	1.817	0.00481	0.0664	9.56	0.398
I - 3	340	1.817	0.00484	0.0664	9.10	0.421
II - 1	300	1.817	0.01179	0.0664	7.43	0.796
II - 2	320	1.817	0.01177	0.0664	7.82	0.836
II - 3	340	1.817	0.01175	0.0664	8.31	0.882
III - 1	300	1.817	0.0251	0.0664	3.69	0.842
III - 2	320	1.817	0.02497	0.0664	3.90	0.884
III - 3	340	1.817	0.0253	0.0664	4.15	0.932
IV - 1	300	2.975	0.00628	0.0906	8.43	0.481
IV - 2	320	2.975	0.00632	0.0906	8.89	0.511
IV - 3	340	2.975	0.00639	0.0906	9.41	0.552
V - 1	300	3.925	0.007125	0.1029	7.76	0.503
V - 2	320	3.925	0.00724	0.1029	8.06	0.531
V - 3	340	3.925	0.00720	0.1029	8.86	0.580

Reproduced with permission of the copyright owner. Further reproduction prohibited without permission.

Table - 1 (Cont'd)

Experimental Results of Oxidation Runs

Run No.	Temperature °C	Total Pressure Atm.	Flow Rate lb-moles/hr.		Conversion %	Rate of Reaction
			Methane	Oxygen	$\frac{\text{lb-moles } CH_4 \text{ converted}}{\text{lb-moles } CH_4 \text{ in feed}} \times 100$	$\frac{\text{lb-moles } CH_4 \text{ converted}}{\text{(hr.)(lb. of catalyst)}}$
VI - 1	300	5.22	0.00816	0.1173	7.54	0.559
VI - 2	320	5.22	0.00812	0.1173	7.89	0.581
VI - 3	340	5.22	0.00819	0.1173	8.60	0.640
VII - 1	300	6.24	0.0088	0.1270	7.42	0.594
VII - 2	320	6.24	0.0087	0.1270	7.74	0.616
VII - 3	340	6.24	0.00886	0.1270	8.36	0.673
VIII - 1	300	7.13	0.00961	0.1392	7.15	0.624
VIII - 2	320	7.13	0.00958	0.1392	7.57	0.658
VIII - 3	340	7.13	0.00971	0.1392	8.16	0.720
IX - 1	300	8.41	0.01117	0.1610	6.45	0.655
IX - 2	320	8.41	0.01123	0.1610	6.80	0.694
IX - 3	340	8.41	0.0112	0.1610	7.41	0.745
X - 1	300	9.70	0.01231	0.1753	5.99	0.671
X - 2	320	9.70	0.01225	0.1753	6.39	0.712
X - 3	340	9.70	0.01232	0.1753	6.89	0.771

CHAPTER VI

ANALYSIS OF RESULTS

In the interpretation of experimental kinetic data, many experimental errors might be encountered. A detailed consideration of the errors that might affect the observed rate of reaction is essential to a valid interpretation of experimental results. Hougen[24] has discussed these errors, arranged below in the order of decreasing importance:

1. Variation in catalyst activity.
2. Departure from unity in effectiveness factor of catalyst.
3. External resistance due to mass and heat transfer.
4. Neglect of pressure drop due to flow.
   Besides these, the following sources of experimental errors should also be considered.
5. Side reactions.
6. Homogenised reaction and catalyzed reaction by reactor wall.
7. Errors associated with analysis, flow measurement and temperature measurement.

1. Variation in Catalyst Activity

Mezaki[18], who used the same catalyst as the one employed in this investigation, reported that catalyst activity decreases considerably during the twenty hour service period. After this period the activity reached a fairly constant value. Therefore for each series of runs, the catalyst was first allowed to attain uniform activity.

Reproduced with permission of the copyright owner. Further reproduction prohibited without permission.

2. Departure from unity in effectiveness factor of Catalyst

The effectiveness factor of a catalyst pellet is defined by Hougen[24] as follows:

"The effectiveness factor of a catalyst pellet is the ratio of the actual reaction rate per unit mass of catalyst when the catalyst is distributed throughout a porous pellet to the rate where the available catalyst is restricted to the exterior surface of the surface." The catalyst used in this investigation consisted of small pellets, 1/8" x 1/8". In this catalyst, the penetration of palladium into alumina pallets was only superficial. The most active part of the catalyst was distributed on the surface or located near enough the surface. Therefore, it was assumed that the effectiveness factor was very close to unity.

3. External resistance due to mass and heat transfer

Yang and Hougen[22] have detailed the equations for calculating heat and mass transfer effects for different operating conditions. The calculations for run 1 - I are given in Appendix III.

Results of these calculations indicate that for all runs, the heat and mass transfer effects were negligible.

4. Neglect of pressure drop due to flow

To take into account pressure drop due to flow, the operating pressure was taken as the mean of reactor inlet and outlet pressures.

Reproduced with permission of the copyright owner. Further reproduction prohibited without permission.

5. Side reactions

In the trial runs over the range of operating conditions, no side products were detected by the chromatographic analysis.

6. Homogenized reaction and catalyzed reaction by reactor walls

In the blank runs over the range of operating conditions, no reaction products were detected by the chromatographic analysis.

7. Errors associated with analysis, flow measurement and temperature measurement

The errors due to analysis of feed streams and product streams were less than 0.5%. The errors due to flow measurement and temperature measurement were negligible.

KINETIC INTERPRETATION OF RESULTS

The interpretation of the initial rate results consists usually of two parts, first, a qualitative interpretation based on the nature of results obtained, and second, a statistical interpretation to obtain a quantitative rate expression. The acceptability criteria for statistical interpretation is that for any rate equation, all equilibrium constants have to be positive. The various plausible mechanisms for the reaction are given in Table 2.

The initial rates obtained in this experimental study were plotted against the total pressure value. The plots for the three temperatures 300, 320 and 340°C are given in figures 3, 4 and 5.

Reproduced with permission of the copyright owner. Further reproduction prohibited without permission.

Reproduced with permission of the copyright owner. Further reproduction prohibited without permission.

TABLE 2(a) INITIAL RATE EQUATIONS FOR PROBABLE MECHANISMS

REACTION	REACTION MECHANISM	RATE CONTROLLING STEP			
		a) ADSORPTION of OXYGEN	b) SURFACE REACTION	c) DESORPTION of PRODUCTS	d) ABSORPTION of METHANE
I	Adsorbed oxygen, methane, carbon dioxide and water. Oxygen dissociated and adsorbed, Surface reaction: $CH_4l + 4Ol \rightleftharpoons CO_2l + 2H_2Ol + 2l$	$a\pi^2/(1+b\pi)^4$	$a\pi^3/(1+b\pi + c\sqrt{\pi})^5$	C	$\frac{a\pi}{(1+b\sqrt{\pi})}$
II	Adsorbed oxygen, methane, carbon dioxide and water. Oxygen not dissociated and adsorbed on (i) dual sites (ii) single sites Surface reaction: $2O_2l + CH_4l \rightleftharpoons CO_2l + 2H_2Ol$	i) $\frac{a\pi^2}{(1+b\pi)^4}$ ii) $\frac{a\pi^2}{(1+b\pi)^2}$	$a\pi^3/(1+b\pi)^3$	C	$\frac{a\pi}{(1+b\pi)}$
III	Methane in gas phase, oxygen dissociated and adsorbed on dual sites or single sites (i) both products adsorbed (ii). One of the products adsorbed (iii) both the products in gas phase Surface reaction: $4Ol + CH_4 \rightleftharpoons CO_2l + 2H_2Ol + l$	$C\pi^2$	$a\pi^3/(1+b\sqrt{\pi})^4$	C	-
IV	Methane in gas phase, oxygen not dissociated and adsorbed on dual sites or single sites (i). One of the products adsorbed (ii) both the products in gas phase Surface reaction: $2O_2l + CH_4 \rightleftharpoons 2H_2O_l + CO_2$	$C\pi^2$	$a\pi^3/(1+b\pi)^2$	C	-
V	Oxygen in gas phase, methane adsorbed molecularly (i) Carbon dioxide adsorbed (ii) Both products in gas phase $2O_2 + CH_4l \rightleftharpoons 2H_2O + CO_2l$	-	$a\pi^3/(1+b\pi)$	C	$C\pi$

TABLE 2(b) DESIGNATION OF INITIAL RATE EQUATIONS

INITIAL RATE EQUATION NO.	REACTIONS	INITIAL RATE EQUATION
(I)	II a (ii)	$a\pi^2/(1 + b\pi)^2$
(II)	II b	$a\pi^3/(1 + b\pi)^3$
(III)	IV b	$a\pi^3/(1 + b\pi)^2$
(IV)	V b	$a\pi^3/(1 + b\pi)$
(V)	II d	$a\pi/(1 + b\pi)$
(VI)	Ia, II a (i)	$a\pi^2/(1 + b\pi)^4$
(VII)	III b	$a\pi^3/(1 + b\sqrt{\pi})^4$
(VIII)	I d	$a\pi/(1 + b\sqrt{\pi})$
(IX)	I b	$a\pi^3/(1 + b\pi + C\sqrt{\pi})^5$
(X)	Ic, IIc, IIIc, IVc, Vc	C
(XI)	V d	$C\pi$
(XII)	IIIa, IVa	$C\pi^2$

Reproduced with permission of the copyright owner. Further reproduction prohibited without permission.

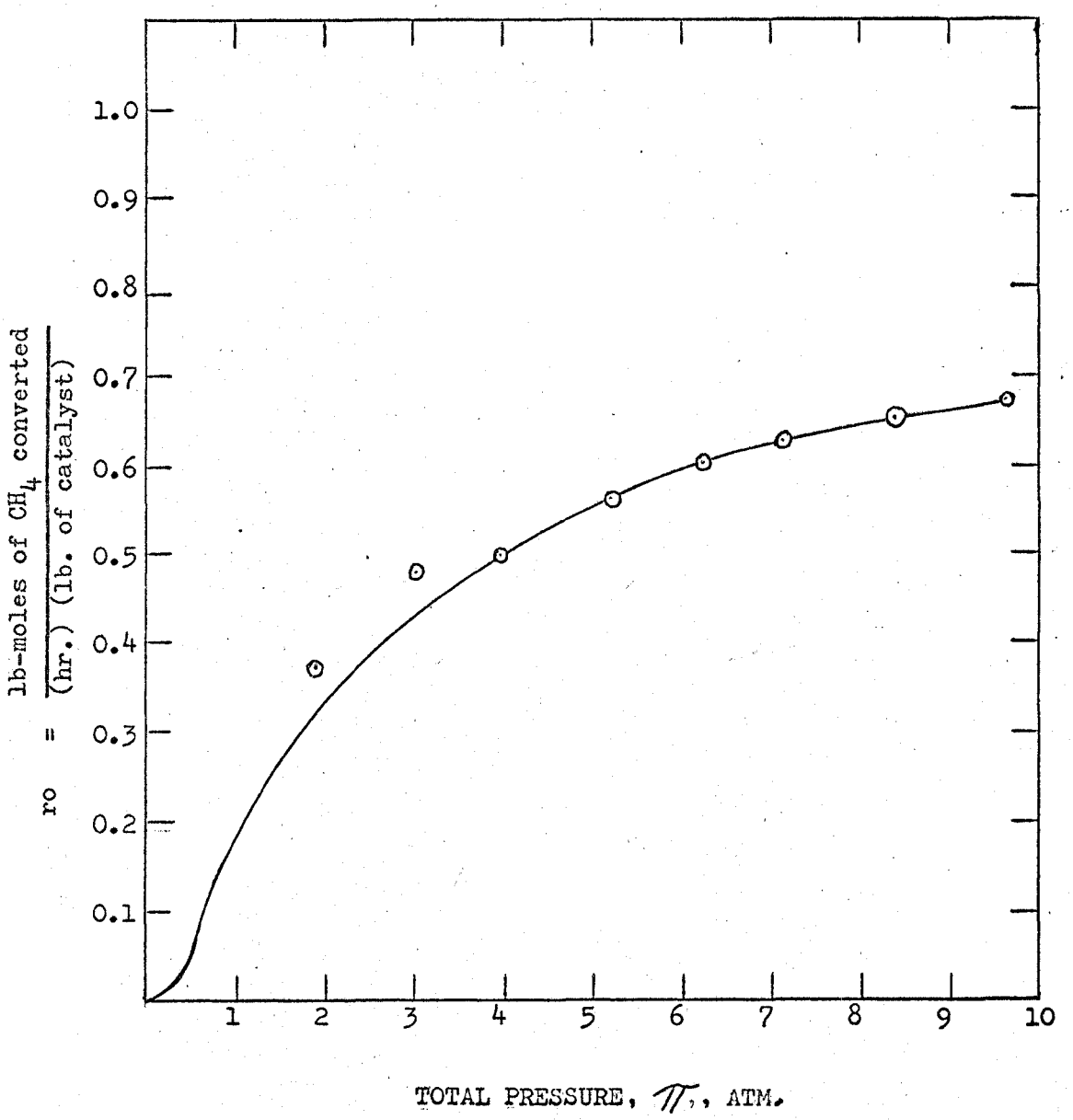

Fig. 3 INITIAL RATE OF REACTION VS TOTAL PRESSURE, 300°C

Reproduced with permission of the copyright owner. Further reproduction prohibited without permission.

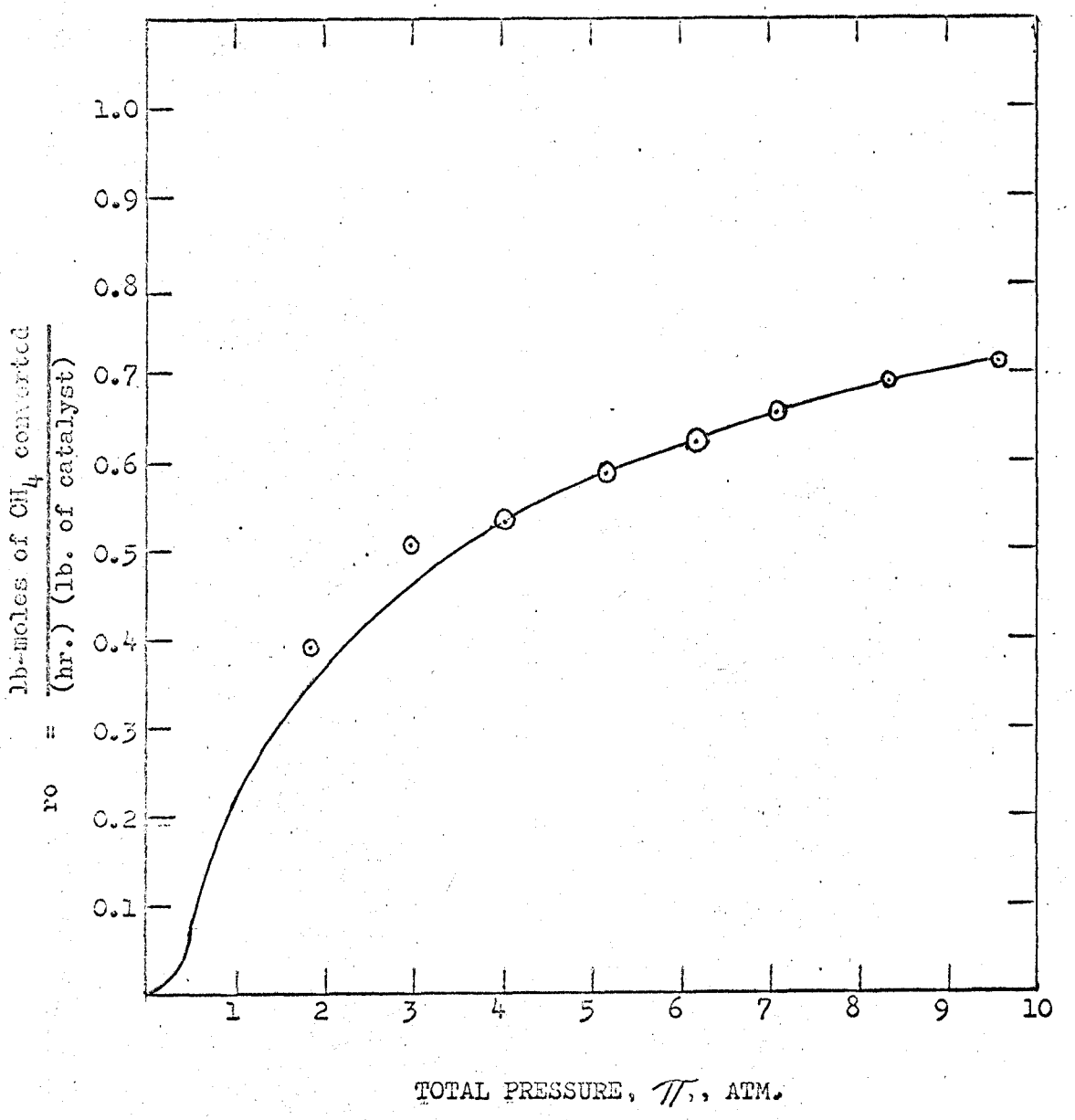

Fig. 4 INITIAL RATE OF REACTION VS TOTAL PRESSURE, 320°C

Reproduced with permission of the copyright owner. Further reproduction prohibited without permission.

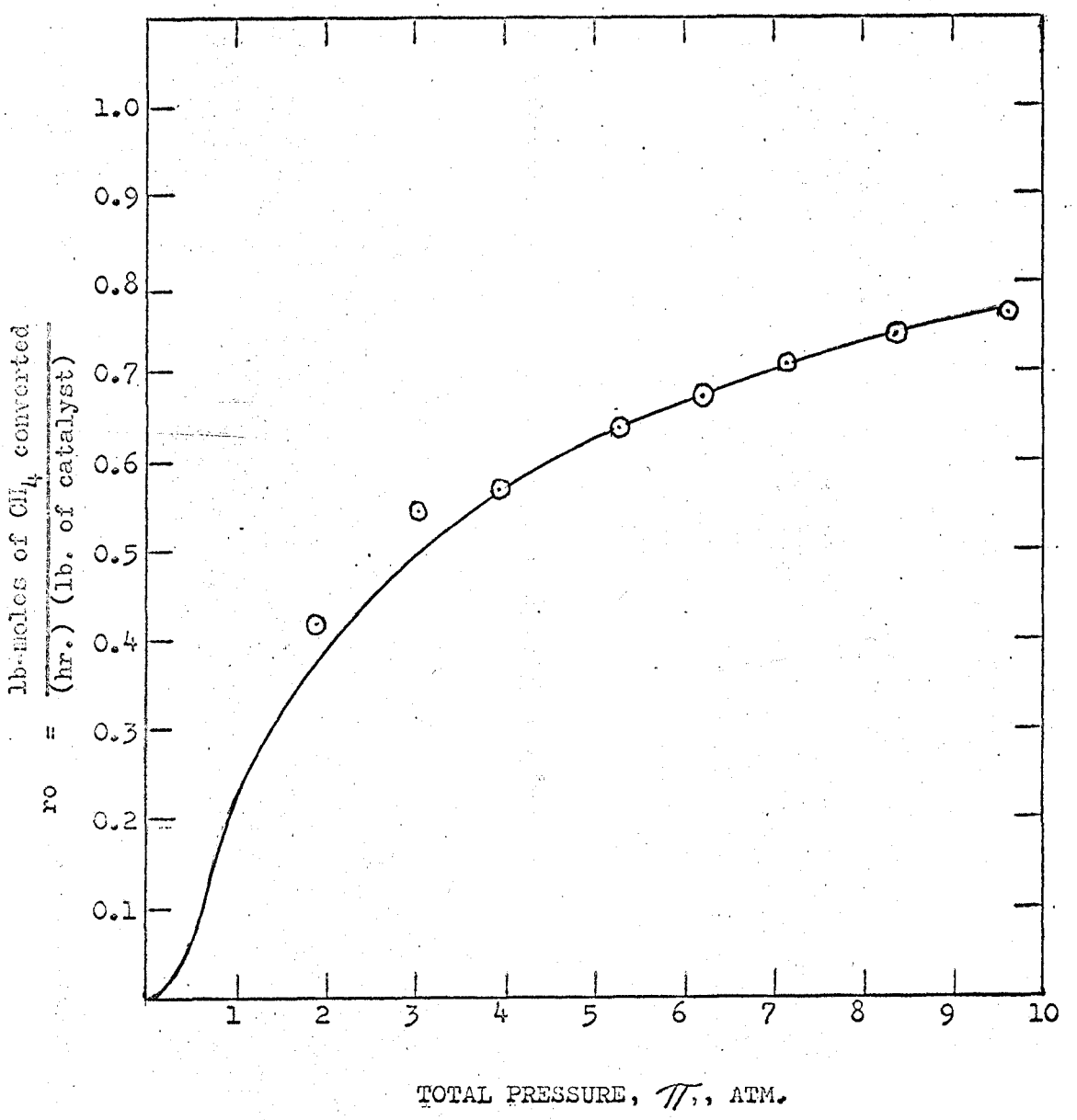

Fig. 5 INITIAL RATE OF REACTION VS TOTAL PRESSURE, 340°C

Reproduced with permission of the copyright owner. Further reproduction prohibited without permission.

From these figures, the reaction mechanisms represented by equations ro C, $ro = C\pi$ and $ro = C\pi^2$ can be rejected, as their plots would be grossly different from the plots of figures 3, 4 and 5.

To examine the validity of other possibilities, coefficients of the remaining nine theoretical rate equations were estimated from the experimental data for three temperatures. The non-linear rate equations were transformed to linear equations by algebric manipulation. The coefficients of these linearised rate equations were estimated from the statistical methods of linear regression.[25] Considering the rate equation (I)

$$ro = a\pi^2 / (1 + b\pi)^2$$

Rearranging, this becomes

$$\frac{\pi}{(ro)^{1/2}} = \frac{1}{(a)^{1/2}} + \frac{b}{(a)^{1/2}} \pi$$

or, an expression of the type $Y = A + BX$

The regression coefficients A and B are given by

$$A = \frac{\Sigma X^2 \Sigma Y - \Sigma X \Sigma XY}{n \Sigma X^2 - (\Sigma X)^2}$$

$$B = \frac{n \Sigma XY - \Sigma X \Sigma Y}{n \Sigma X^2 - (\Sigma X)^2}$$

For an expression involving three coefficients, as in case of rate equation (IX)

$$ro = \frac{a\pi^3}{(1 + b\pi + C\sqrt{\pi})^5}$$

Rearranging, this becomes

$$\frac{\pi^{3/5}}{(ro)^{1/5}} = \frac{1}{(a)^{1/5}} + \frac{b}{(a)^{1/5}}\pi + \frac{C}{(a)^{1/5}}\sqrt{\pi}$$

Reproduced with permission of the copyright owner. Further reproduction prohibited without permission.

or, an expression of the type $Z = B_0 + B_1X + B_2Y$

The coefficients B_0, B_1 and B_2 are given by three linear equations computed by the method of multiple regression[25]

$$\Sigma Z = n B_0 + B_1 \Sigma X + B_2 \Sigma Y$$
$$\Sigma XZ = B_0 \Sigma X + B_1 \Sigma X^2 + B_2 \Sigma XY$$
$$\Sigma YZ = B_0 \Sigma Y + B_1 \Sigma XY + B_2 \Sigma Y^2$$

The coefficients of nine equations were computed on an IBM-1620 computer. The programmes and results are given in Appendix V. The results are tabulated in Table 3.

From the nature of the plots in figures 3, 4 and 5, no shift in mechanism was noted over the temperature range 300, 320 and 340°C. Moreover, none of the figures 3, 4 and 5 showed a maxima. Therefore, the possibility of the reaction mechanism given by rate equation (VI), which exhibits a maxima for π max. $= \frac{1}{b}$, was rejected. The rate equations (III) and (IV) depicted negative regression coefficients, so these were also excluded as plausible mechanisms.

Rate equations I, II, V, VII, VIII and IX showed positive values for regression coefficients and remained possible mechanisms. These six possible equations were then subjected to goodness of fit criteria. Equations VII, VIII and IX showed a variation of more than 100% from experimental values of initial rates, thus eliminating them as possible mechanistic equations. Equations I, II and V showed an average variation of 1% from experimental data.

Reproduced with permission of the copyright owner. Further reproduction prohibited without permission.

TABLE 3 REGRESSION COEFFICIENTS FOR LINEARISED RATE EQUATIONS

Rate Equation No.	Mechanism designation	Initial rate Equation	Regression Coefficients			VALUE OF REGRESSION COEFFICIENT								
						300°C			320°C			340°C		
			A	B	C	A	B	C	A	B	C	A	B	C
(I)	IIa (ii)	$ro = a\pi^2/(1 + b\pi)^2$	$\frac{1}{a^{\frac{1}{2}}}$	$\frac{b}{a^{\frac{1}{2}}}$	-	1.0341	1.1199	-	1.0186	1.0889	-	0.9739	1.0456	-
(II)	IIb	$ro = a\pi^3/(1 + b\pi)^3$	$\frac{1}{a^{\frac{1}{2}}}$	$\frac{b}{a^{1/3}}$	-	0.6227	1.0820	-	0.6196	1.0619	-	0.5995	1.0337	-
(III)	IVb	$ro = a\pi^3/(1 + b\pi)^2$	$\frac{1}{a^{\frac{1}{2}}}$	$\frac{b}{a^{\frac{1}{2}}}$	-	-4.9805	4.1727	-	4.7978	4.0551	-	4.6422	3.8980	-
(IV)	Vb	$ro = a\pi^3/(1 + b\pi)$	$\frac{1}{a}$	$\frac{b}{a}$	-	-471.924	164.676	-	-443.534	155.399	-	-411.557	143.724	-
(V)	IId	$ro = a\pi/(1 + b\pi)$	$\frac{1}{a}$	$\frac{b}{a}$	-	2.8184	1.2083	-	2.6924	1.1434	-	2.4848	1.0523	-
(VI)	Ia, IIa(i)	$ro = a\pi^2/(1 + b\pi)^4$	$\frac{1}{a^{\frac{1}{4}}}$	$\frac{b}{a^{\frac{1}{4}}}$	-	1.4481	0.2140	-	1.4292	0.2112	-	1.4021	0.2066	-
(VII)	IIIb	$ro = a\pi^3/(1 + b\sqrt{\pi})^4$	$\frac{1}{a^{\frac{1}{4}}}$	$\frac{b}{a^{\frac{1}{4}}}$	-	1.2189	0.5118	-	1.2051	0.5048	-	1.1809	0.4944	-
(VIII)	Id	$ro = a\pi/(1 + b\sqrt{\pi})$	$\frac{1}{a}$	$\frac{b}{a}$	-	2.8184	1.2083	-	2.6925	1.1434	-	2.4848	1.0523	-
(IX)	Ib	$ro = a\pi^3/(1 + b\pi + c\sqrt{\pi})^5$	$\frac{1}{a^{1/5}}$	$\frac{b}{a^{1/5}}$	$\frac{c}{a^{1/5}}$	0.1007	0.06061	1.1383	0.1061	0.06126	1.1018	0.1151	0.06916	1.0936

Reproduced with permission of the copyright owner. Further reproduction prohibited without permission.

As proposed by Yang and Hougen[22], the effect of feed composition upon rate of reaction was utilised to eliminate further implausible mechanisms. Plots of rate of reaction against methane percent in feed composition are given by figures 6, 7 and 8. Interpretation from these plots, rules out the survival of reaction mechanisms given by equations I and V. The plots of equations I and V would be entirely different from the plots of figures 6, 7 and 8.

Further more, as a check, values of initial rates from equations I, II and V were computed for the varying feed composition runs, by using the corresponding linear regression coefficients. The experimental data showed a variation of more than 100% from that predicted by equation I, about 25% from that predicted by equation V, only about 4% from that obtained by equation II.

Hence, from qualitative view points, equation II is the probable mechanism for methane oxidation. Also, from quantitative interpretations, it is the most accurate fit both for constant feed and varying feed composition runs.

Therefore, it is proposed that following is the rate controlling mechanism for methane oxidation.

" Oxygen and methane adsorbed on the catalyst surface, the surface is:

$$2\ O_2l + CH_4l \rightleftharpoons 2\ H_2Ol + CO_2l$$

surface reaction is rate controlling ".

Reproduced with permission of the copyright owner. Further reproduction prohibited without permission.

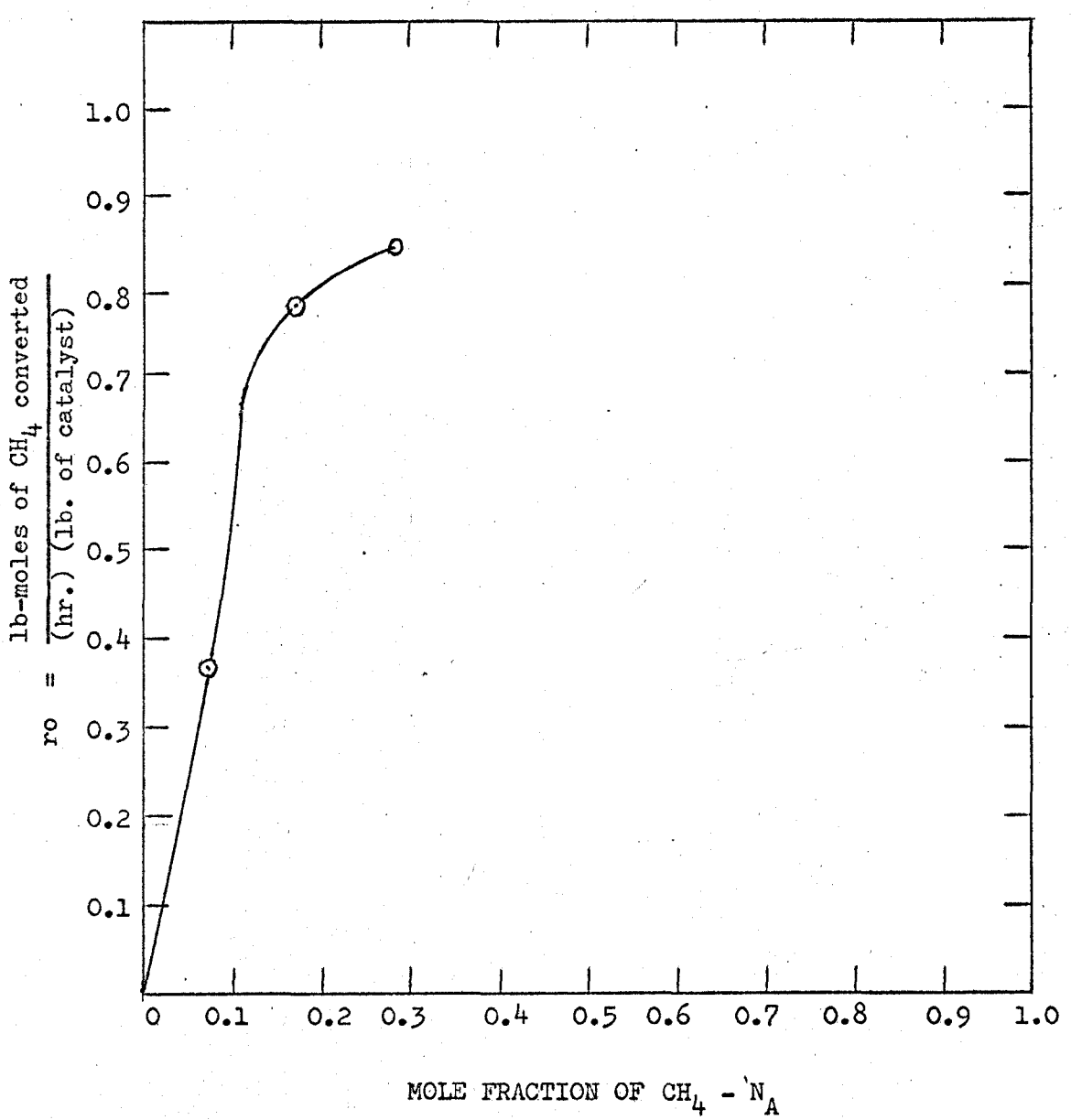

Fig. 6 INITIAL RATE OF REACTION VS FEED COMPOSITION, 300°C, 1.817 ATM.

Reproduced with permission of the copyright owner. Further reproduction prohibited without permission.

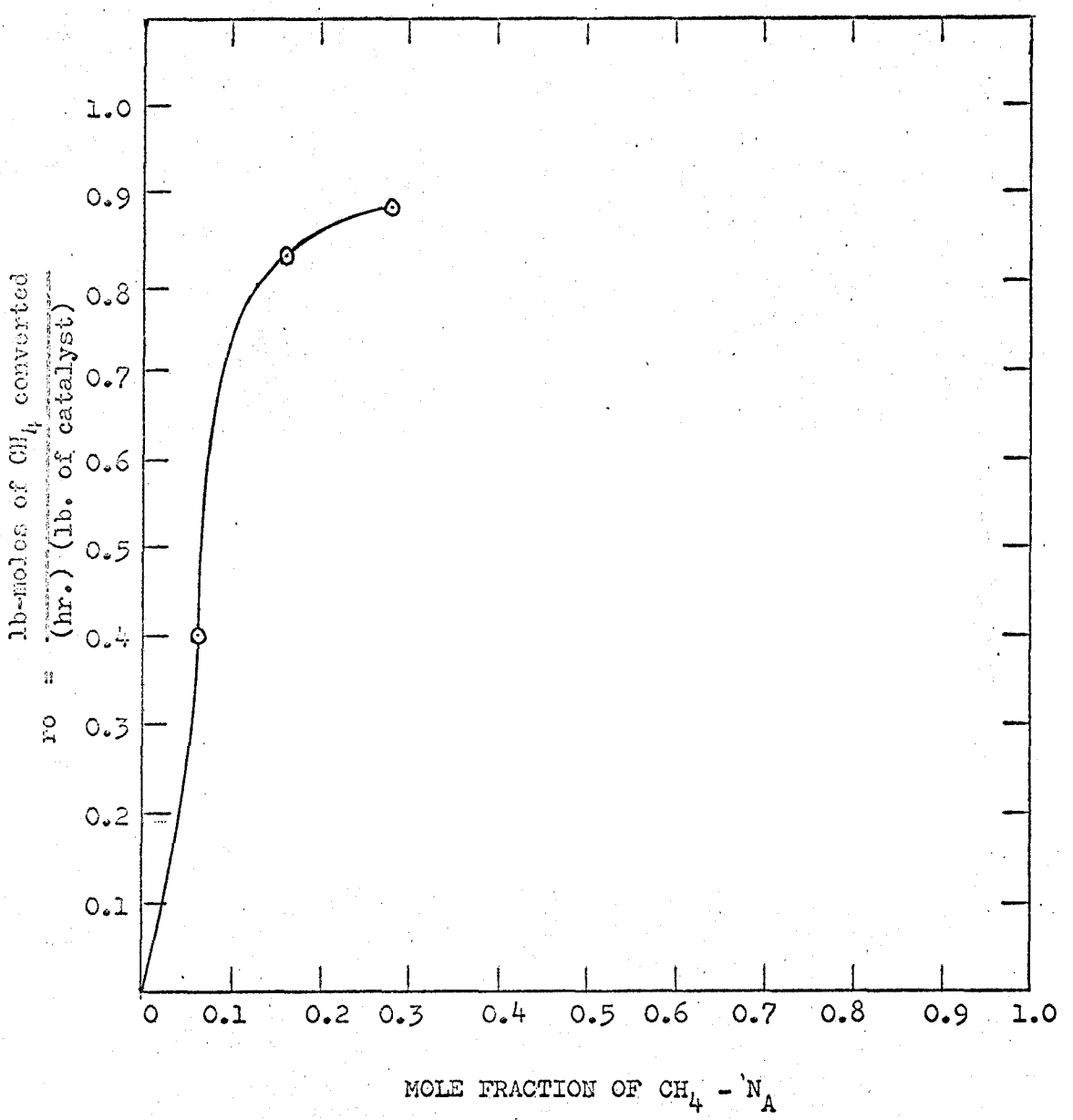

Fig. 7 INITIAL RATE OF REACTION VS FEED COMPOSITION, 320°C, 1.817 ATM.

Reproduced with permission of the copyright owner. Further reproduction prohibited without permission.

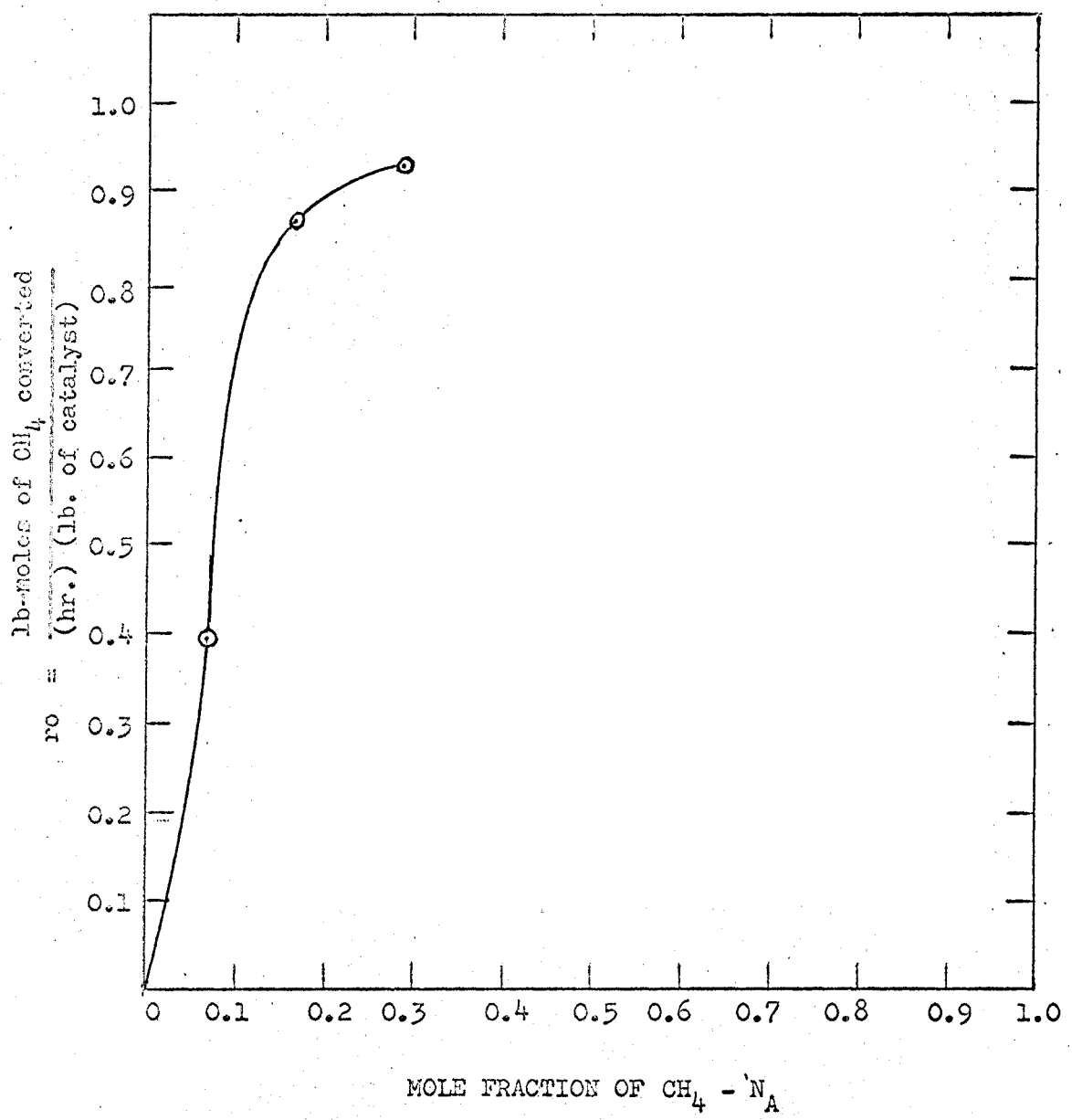

Fig. 8 INITIAL RATE OF REACTION VS FEED COMPOSITION, 340°C, 1.817 ATM.

Reproduced with permission of the copyright owner. Further reproduction prohibited without permission.

The corresponding rate equation has the form

$$r = \frac{C\left[p_{CH_4}\, p^2_{O_2} - p^2_{H_2O}\, p_{CO_2} / K\right]}{\left[1 + K_{CH_4}\, p_{CH_4} + K_{O_2}\, p_{O_2} + K_{CO_2}\, p_{CO_2} + K_{H_2O}\, p_{H_2O}\right]^3}$$

the corresponding initial rate equation is:

$$ro = a\,\pi^3 / (1 + b\pi)^3$$

at 300°C $\quad ro = 4.144\,\pi^3 / (1 + 1.737\pi)^3$

at 320°C $\quad ro = 4.206\,\pi^3 / (1 + 1.714\pi)^3$

at 340°C $\quad ro = 4.644\,\pi^3 / (1 + 1.723\pi)^3$

The initial rates computed from the proposed mechanistic equation and their variation from experimental data are given in Table 4.

Figures 9, 10 and 11 graphically illustrate the agreement of the computed rates with the observed reaction rate.

Mezaki's rate equation gives a deviation of about 17%, as compared to the deviation of 4% based on the equation arrived at in this investigation. Table 4-a gives the results based on proposed mechanistic equation as compared to results based on Mezaki's investigation.

Reproduced with permission of the copyright owner. Further reproduction prohibited without permission.

Reproduced with permission of the copyright owner. Further reproduction prohibited without permission.

Table - 4

Mechanistic Rate Equation Data

A. Constant Feed Composition runs at 300°C

$a = 4.144$ $b = 1.737$

Run No.	Total Pressure Atm. (π)	Rate of Reaction Experimental	Rate of Reaction from $Ro = a\pi^3/(1 + b\pi)^3$	% Variation from Experimental value
I - 1	1.817	0.373	0.3463	+ 7.16
IV - 1	2.975	0.481	0.4652	+ 3.28
V - 1	3.925	0.503	0.5245	- 4.27
VI - 1	5.22	0.559	0.5833	- 4.34
VII - 1	6.24	0.594	0.6068	- 2.15
VIII - 1	7.13	0.624	0.6262	- 0.35
IX - 1	8.41	0.655	0.6494	+ 0.85
X - 1	9.70	0.671	0.6661	- 0.73

Average = 0.55%

B. Varying Feed Composition runs at 300°C, 1.817 Atm.; $a' = 71.38$, $b' = 1.737$

Run No.	Mole Fraction of Methane in Feed	Rate of Reaction Experimental	Rate of Reaction from $Ro = \dfrac{a'[p_{CH_4}][p_{O_2}]^2}{[1 + b'(p_{CH_4} + p_{O_2})]^3}$	% Variation from Experimental value
I - 1	0.06669	0.373	0.3463	+ 7.16
II - 1	0.1517	0.796	0.723	+ 9.17
III - 1	0.2806	0.842	0.863	- 2.49

Average = 4.61%

Reproduced with permission of the copyright owner. Further reproduction prohibited without permission.

Table 4 - (Cont'd) Mechanistic Rate Equation Data

A. Constant Feed Composition Runs at 320°C

$a = 4.206$ $b = 1.714$

Run No.	Total Pressure Atm. (π)	Rate of Reaction Experimental	Rate of Reaction from $Ro = a\pi^3 / (1 + b\pi)^3$	% variation from Experimental value
I - 2	1.817	0.398	0.362	+ 9.04
IV - 2	2.975	0.511	0.488	+ 4.50
V - 2	3.925	0.531	0.5511	- 3.78
VI - 2	5.22	0.581	0.607	- 4.47
VII - 2	6.24	0.616	0.638	- 3.57
VIII - 2	7.13	0.658	0.660	- 0.30
IX - 2	8.41	0.694	0.6831	- 1.57
X - 2	9.70	0.712	0.7009	- 1.56

Average = 0.20%

B. Varying Feed Composition at 320°C, 1.817 Atm.; $a' = 71.52$ $b' = 1.714$

Run No.	Mole Fraction of Methane in feed	Rate of Reaction Experimental	Rate of Reaction from $Ro = \dfrac{a'[p_{CH_4}][p_{O_2}]^2}{[1 + p_{CH_4} + p_{O_2}]^3}$	% variation from Experimental value
I - 2	0.06765	0.398	0.362	+ 9.04
II - 2	0.1529	0.836	0.775	+ 7.29
III - 2	0.2801	0.884	0.894	- 1.13

Average = 5.06%

Reproduced with permission of the copyright owner. Further reproduction prohibited without permission.

Table 4 - (Cont'd) Mechanistic Rate Equation Data

A. Constant Feed Composition runs at 340°C $a = 4.644$ $b = 1.723$

Run No.	Total Pressure Atm. (π)	Rate of Reaction Experimental	Rate of Reaction from $Ro = a\pi^3 / (1 + b\pi)^3$	% variation from Experimental value
I - 3	1.817	0.421	0.3948	+ 6.22
IV - 3	2.975	0.552	0.5319	+ 3.64
V - 3	3.925	0.580	0.6003	- 3.50
VI - 3	5.22	0.640	0.6615	- 3.35
VII - 3	6.24	0.673	0.6956	- 3.36
VIII - 3	7.13	0.720	0.7188	+ 0.16
IX - 3	8.41	0.745	0.7433	+ 0.228
X - 3	9.70	0.771	0.7631	+ 1.02

Average = 0.13%

B. Varying Feed Composition runs at 340°C, 1.817 Atm. $a' = 78.64$ $b' = 1.723$

Run No.	Mole Fraction of Methane in Feed	Rate of Reaction Experimental	Rate of Reaction from $Ro = \dfrac{a'\left[p_{CH_4}\right]\left[p_{O_2}\right]^2}{\left[1 + b'\left(p_{CH_4} + p_{O_2}\right)\right]^3}$	% variation from Experimental value
I - 3	0.06800	0.421	0.3948	+ 6.22
II - 3	0.1537	0.882	0.829	+ 6.00
III - 3	0.2811	0.932	0.9732	- 4.42

Average = 2.60%

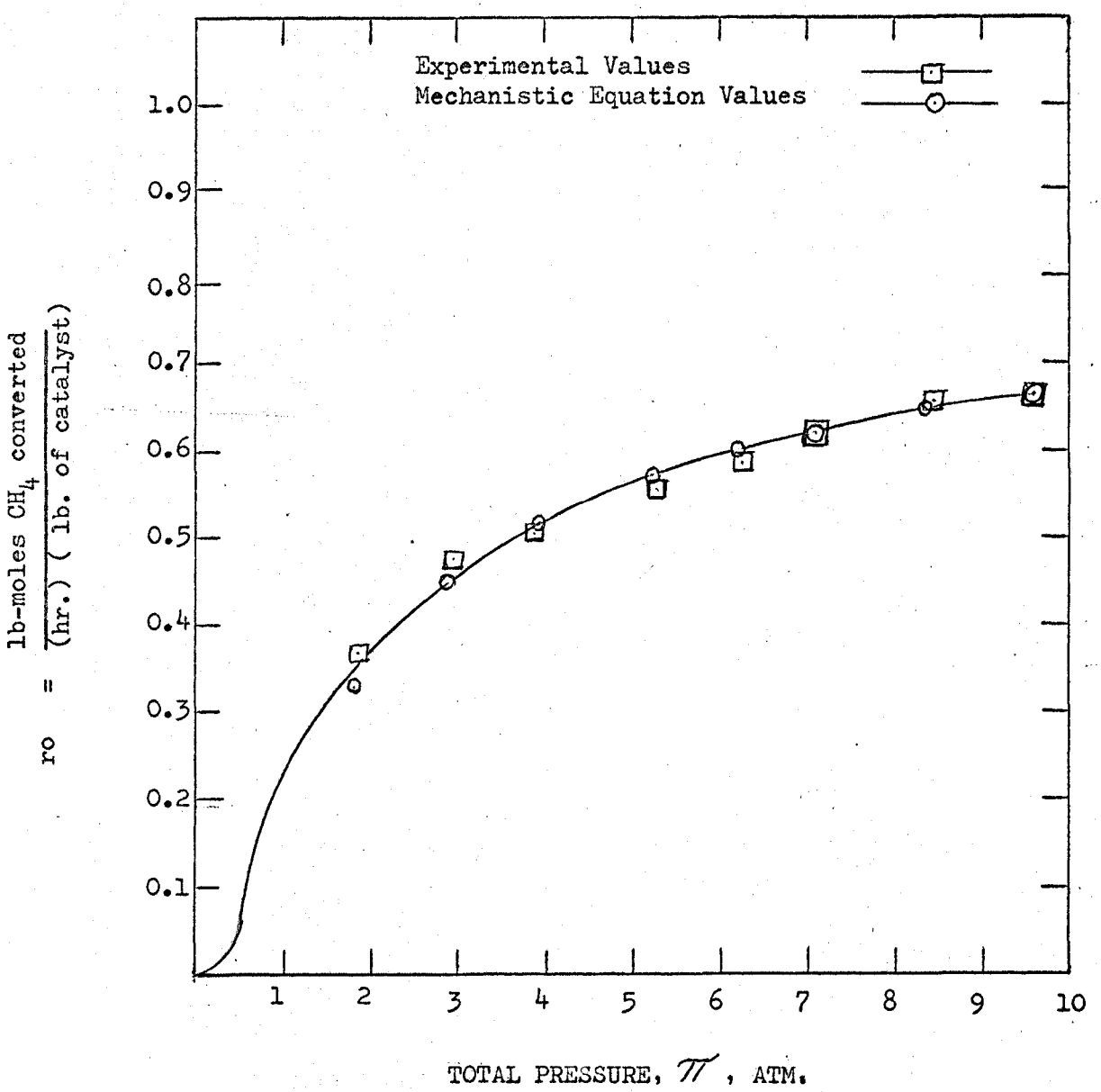

Fig. 9 INITIAL RATE OF REACTION FROM MECHANISTIC EQUATION, 300°C

Reproduced with permission of the copyright owner. Further reproduction prohibited without permission.

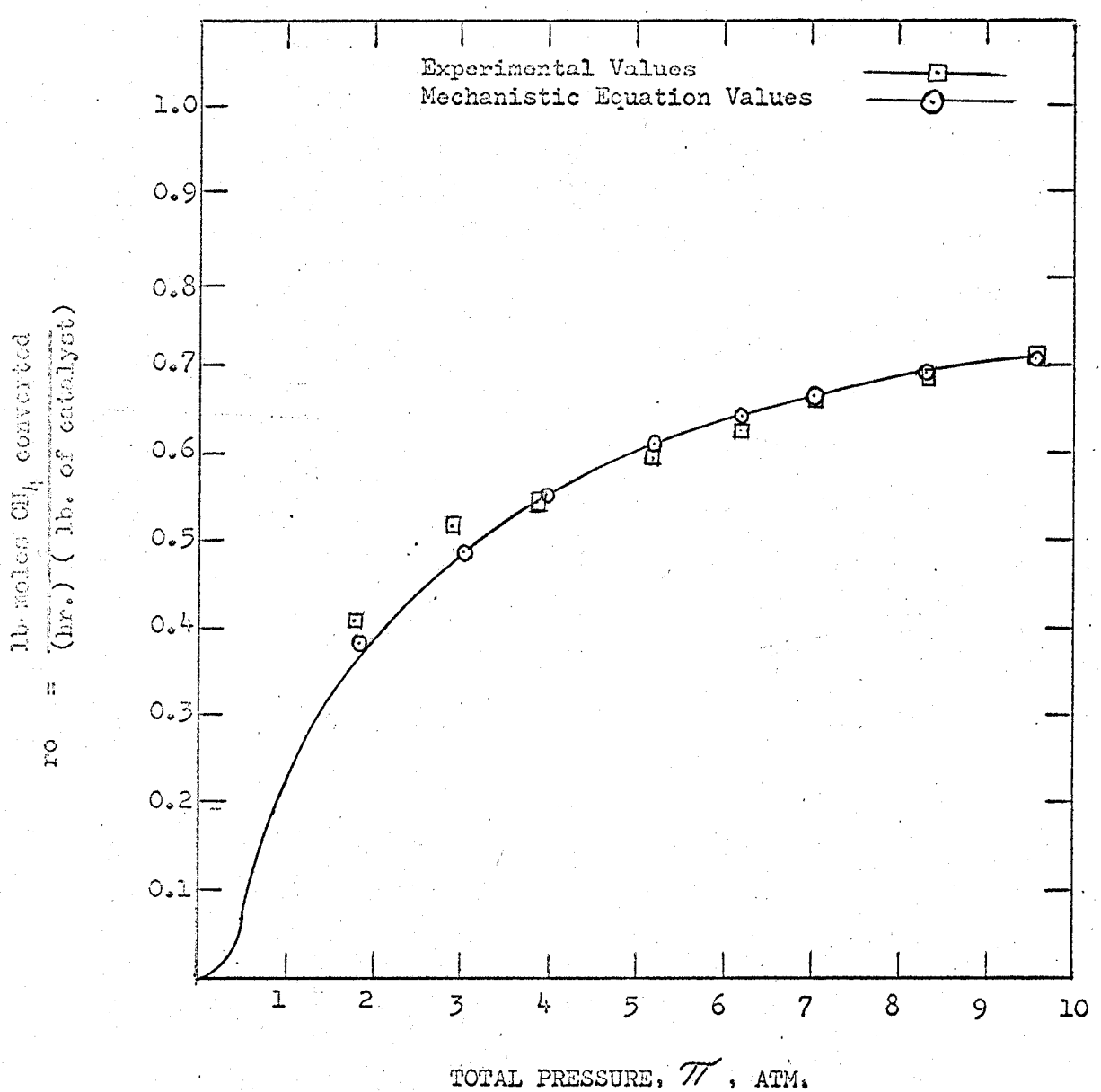

Fig. 10 INITIAL RATE OF REACTION FROM MECHANISTIC EQUATION, 320°C

Reproduced with permission of the copyright owner. Further reproduction prohibited without permission.

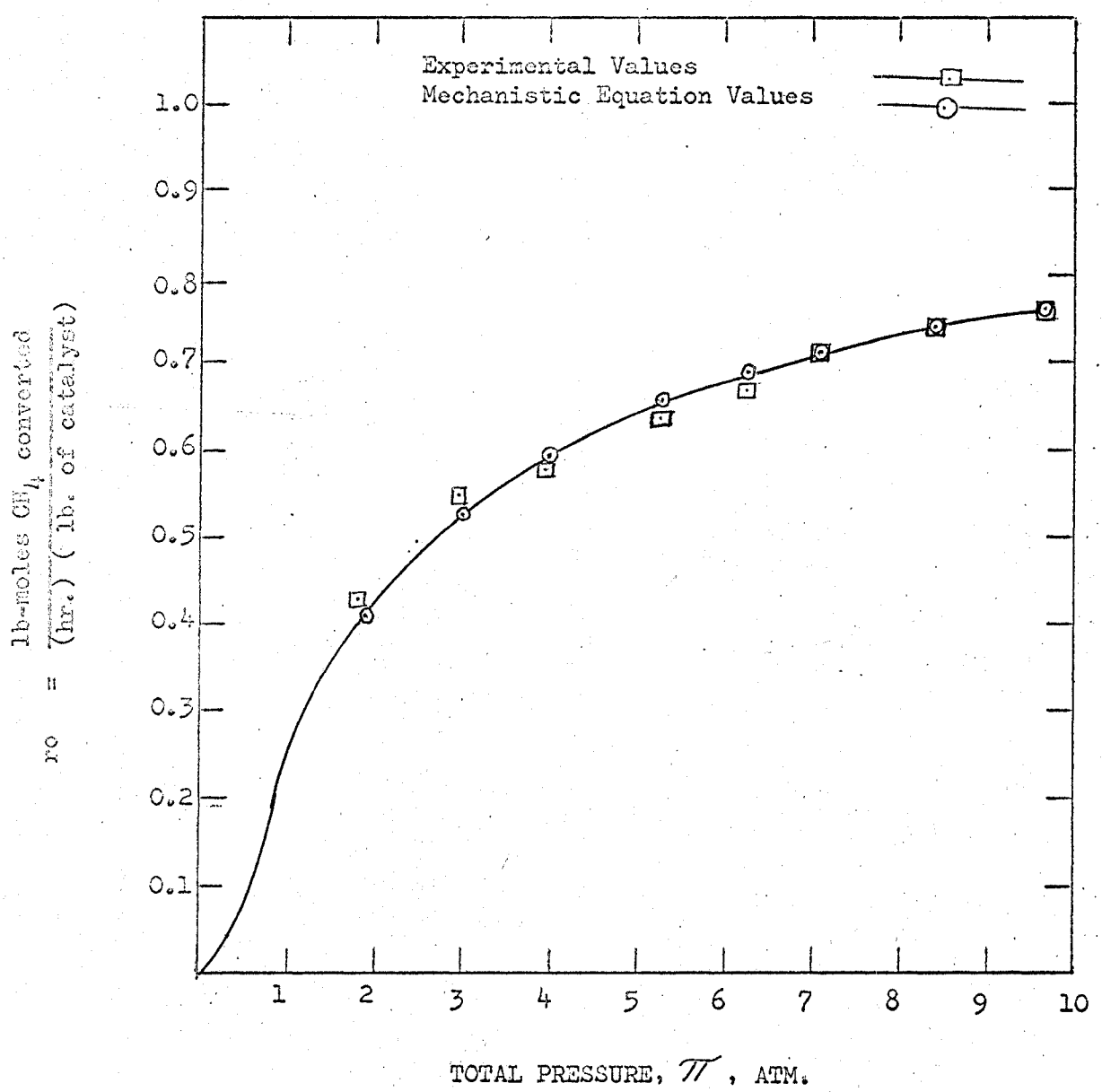

Fig. 11 INITIAL RATE OF REACTION FROM MECHANISTIC EQUATION, 340°C

Reproduced with permission of the copyright owner. Further reproduction prohibited without permission.

Table 4-a

Results of Present Investigation VS Mezaki's Investigation

Temperature	Run No.	ro Experimental Value	Rate of Reaction from $R_o' = \frac{a'[p_{CH_4}][p_{O_2}]^2}{[1 + b'(p_{CH_4} + p_{O_2})]^3}$	% Variation of R_o' from Experimental Value	Rate of Reaction from $R_o'' = \frac{a''[p_{CH_4}][p_{O_2}]^2}{[1 + b''(p_{O_2})]^3}$	% Variation of R_o'' from Experimental Value
300°C	I - 1	0.373	0.3463	+ 7.16	0.296	- 20.8
	II - 1	0.796	0.723	+ 9.17	0.616	- 22.6
	III - 1	0.842	0.863	- 2.49	0.736	- 12.6
				Average 4.61%		Average 15.35%
320°C	I - 2	0.398	0.362	+ 9.04	0.309	- 22.4
	II - 2	0.836	0.836	+ 7.29	0.651	- 22.1
	III - 2	0.884	0.884	- 1.13	0.765	- 13.45
				Average 5.06%		Average 19.32%
340°C	I - 3	0.421	0.421	+ 6.22	0.336	- 20.2
	II - 3	0.882	0.882	+ 6.00	0.709	- 19.6
	III - 3	0.932	0.932	+ 4.42	0.831	- 10.8
				Average 2.60%		Average 16.87%

Reproduced with permission of the copyright owner. Further reproduction prohibited without permission.

EMPIRICAL APPROACH

From the reactor design point of view, it is of interest to subject the oxidation data to a power law model. The following rate equation was used to find the empirical power law coefficients.

$$\text{Rate} = k \left[C_{CH_4}\right]^m \left[C_{O_2}\right]^n \qquad (21)$$

Empirical coefficients for equation (21) were found by multiple regression technique[25]. The computer programme and results are given in Appendix V. The values of empirical coefficients are given in table 5. The average order of reaction was found to be 0.62.

The initial rates computed from the empirical equation (21), and their variation from experimental data, are given in table 5. The average deviation was found to be less than 1%. Figures 12, 13 and 14 graphically illustrate the agreement of computed rates with the observed reaction rates.

The proposed empirical rate equations have the form:

at 300°C, $ro = 2.528 \left[C_{CH_4}\right]^{0.0763} \left[C_{O_2}\right]^{0.5429}$

at 320°C, $ro = 2.635 \left[C_{CH_4}\right]^{0.06726} \left[C_{O_2}\right]^{0.5518}$

at 340°C, $ro = 2.772 \left[C_{CH_4}\right]^{0.05932} \left[C_{O_2}\right]^{0.5613}$

UNIVERSITY OF WINDSOR LIBRARY

Reproduced with permission of the copyright owner. Further reproduction prohibited without permission.

Reproduced with permission of the copyright owner. Further reproduction prohibited without permission.

Table - 5

Empirical Rate Equation Date (300°C)

$m = 0.0763$ $n = 0.5429$ $k = 2.528$

Run No.	Concentration of methane lb-moles C_{CH_4}	Concentration of oxygen lb-moles C_{O_2}	Rate of reaction Experimental	Rate of reaction from $r = [C_{CH_4}]^m [C_{O_2}]^n$	% Variation from Experimental value
I - 1	0.00474	0.0664	0.373	0.3856	- 3.38
II - 1*	0.01179	0.0664	0.796	0.8140	- 2.37
III - 1*	0.0251	0.0664	0.842	0.8557	- 1.63
IV - 1	0.00628	0.0906	0.481	0.4663	+ 3.06
V - 1	0.007125	0.1029	0.503	0.5044	- 0.28
VI - 1	0.008160	0.1173	0.559	0.5473	+ 2.09
VII - 1	0.008800	0.1270	0.594	0.5748	+ 4.91
VIII - 1	0.009610	0.1392	0.624	0.6081	+ 2.55
IX - 1	0.01117	0.1610	0.655	0.6658	- 1.65
X - 1	0.01231	0.1753	0.671	0.7009	- 4.45

Average - 0.11%

Table - 5 (Cont'd)

Empirical Rate Equation Data (320°C)

m = 0.06726 n = 0.5518 k = 2.635

Run No.	Concentration of methane lb-moles C_{CH_4}	Concentration of oxygen lb-moles C_{O_2}	Rate of reaction Experimental	Rate of reaction from $ro = \left[C_{CH_4}\right]^m \left[C_{O_2}\right]^n$	% Variation from Experimental value
I - 2	0.00481	0.0664	0.398	0.4121	- 3.54
II - 2*	0.01177	0.0664	0.836	0.8495	- 1.62
III - 2*	0.02497	0.0664	0.884	0.8677	+ 1.85
IV - 2	0.00632	0.0906	0.511	0.4981	+ 2.52
V - 2	0.00724	0.01029	0.531	0.5394	- 1.58
VI - 2	0.00812	0.01173	0.581	0.5843	- 0.56
VII - 2	0.00877	0.01270	0.616	0.6138	+ 0.36
VIII - 2	0.00958	0.01392	0.658	0.6494	+ 1.31
IX - 2	0.01123	0.01610	0.694	0.7114	+ 2.51
X - 2	0.01225	0.01753	0.712	0.7498	- 5.30

Average - 0.91%

Reproduced with permission of the copyright owner. Further reproduction prohibited without permission.

Reproduced with permission of the copyright owner. Further reproduction prohibited without permission.

Table - 5 (Cont'd)

Empirical Rate Equation Data (340°C)

m = 0.05932 n = 0.5613 k = 2.772

Run No.	Concentration of methane lb-moles C_{CH_4}	Concentration of oxygen lb-moles C_{O_2}	Rate of reaction Experimental	Rate of reaction from $r = \left[C_{CH_4}\right]^m \left[C_{O_2}\right]^n$	% deviation from Experimental value
I - 3	0.00484	0.0664	0.4210	0.4512	- 7.17
II - 3*	0.01175	0.0664	0.882	0.8607	- 2.42
III - 3*	0.02531	0.0664	0.932	0.9473	+ 1.65
IV - 3	0.00639	0.0906	0.552	0.5321	+ 3.60
V - 3	0.00720	0.1029	0.580	0.5772	+ 0.48
VI - 3	0.00819	0.1173	0.640	0.6261	+ 2.17
VII - 3	0.00886	0.1270	0.673	0.6579	+ 2.24
VIII - 3	0.00971	0.1392	0.720	0.6961	+ 3.32
IX - 3	0.0112	0.1610	0.745	0.7619	- 2.27
X - 3	0.01232	0.1753	0.771	0.8037	- 4.24

Average - 0.26%

* Data of these runs not used in plots of initial rate against total pressure, at constant feed composition. These runs have different feed composition

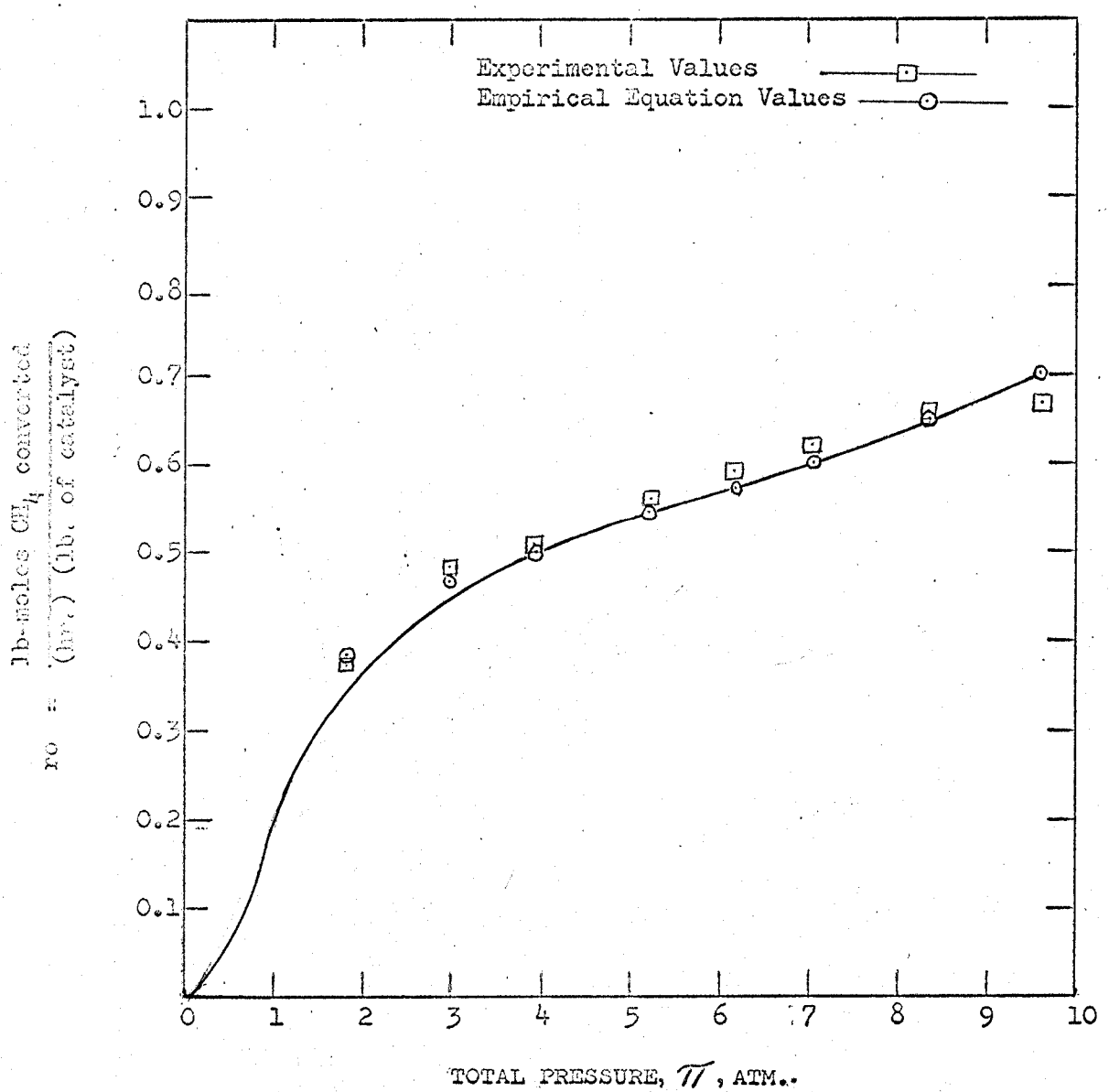

Fig. 12 INITIAL RATE OF REACTION FROM EMPIRICAL EQUATION, 300°C

Reproduced with permission of the copyright owner. Further reproduction prohibited without permission.

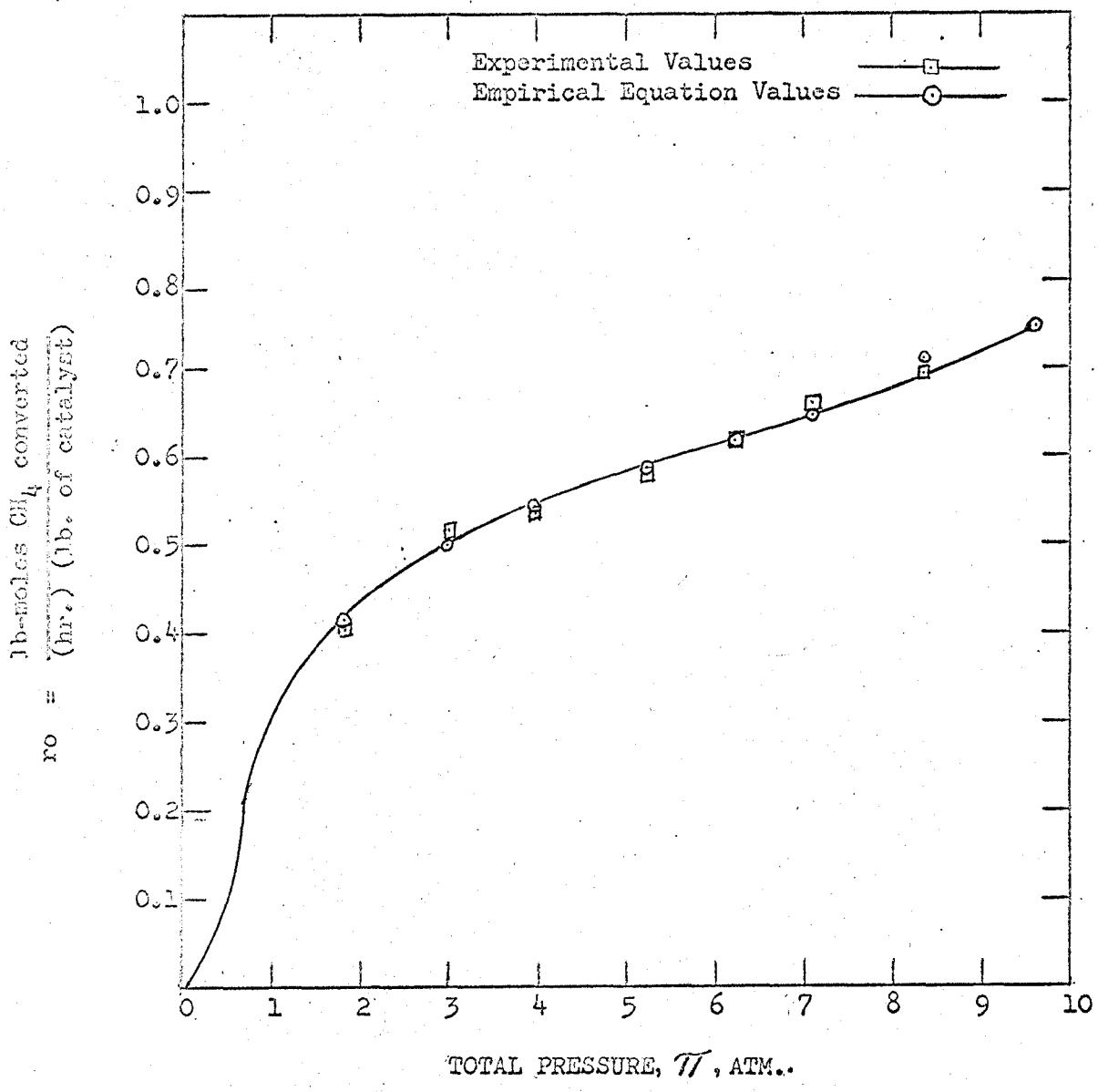

Fig. 13 INITIAL RATE OF REACTION FROM EMPIRICAL EQUATION, 320°C

Reproduced with permission of the copyright owner. Further reproduction prohibited without permission.

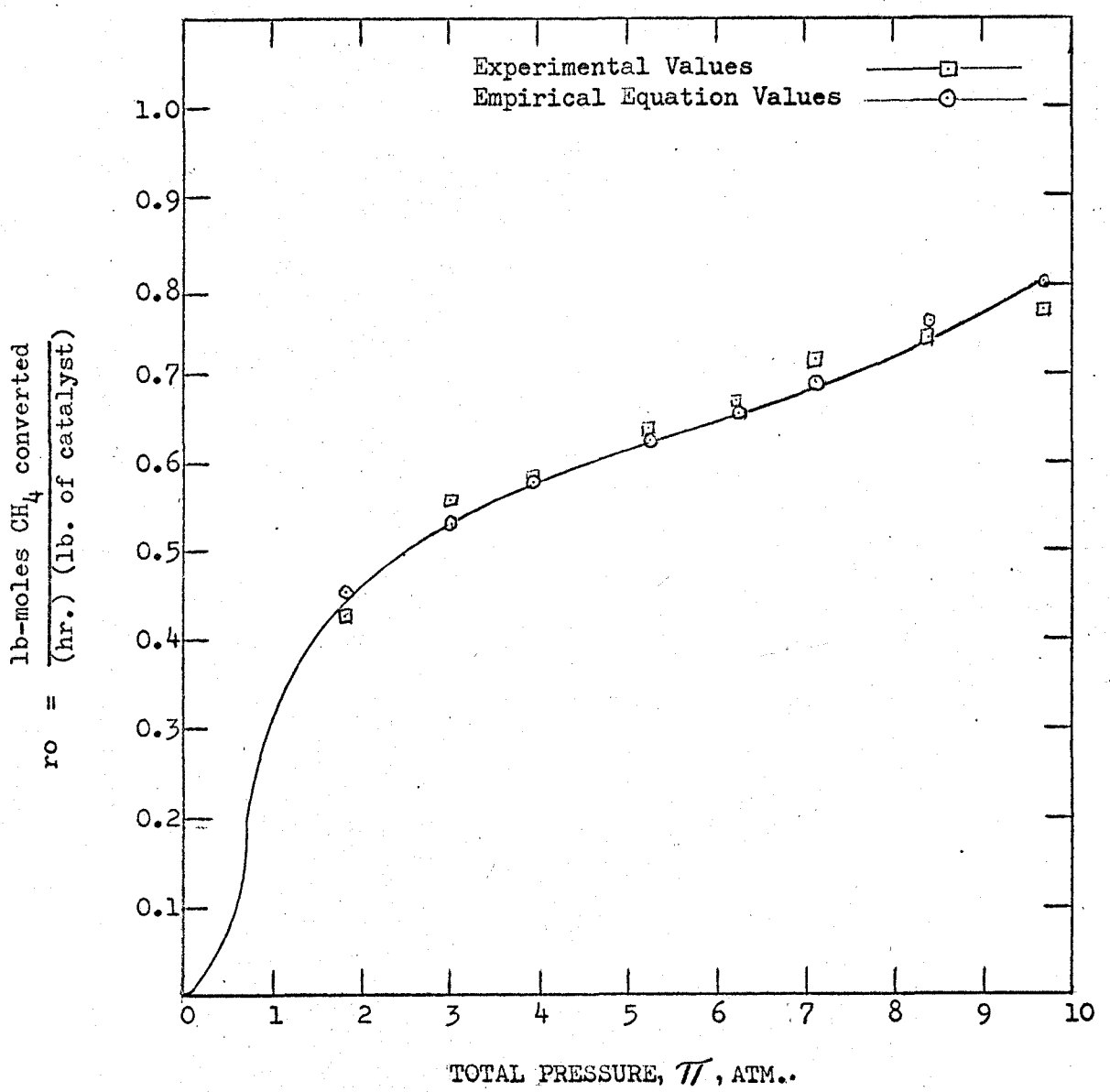

Fig. 14 INITIAL RATE OF REACTION FROM EMPIRICAL EQUATION, 340°C

Reproduced with permission of the copyright owner. Further reproduction prohibited without permission.

CHAPTER VII

CONCLUSIONS

The mechanism for the catalytic oxidation of methane has been established experimentally by applying the inital rate approach.

The plots of initial rate against total pressure gave useful qualitative information and thus some implausible mechanisms could be rejected. The determination of linearised regression coefficients and application of the criteria of best fit was then used to reject mechanisms showing wide variation from experimental data. Negative coefficients for some rate mechanisms also helped to eliminate them as possible mechanisms.

The data of initial rates at varying pressures and constant feed composition was not sufficient to establish the controlling mechanism. Plots of initial rate against varying feed composition served as a very useful tool in finding the controlling mechanism. The experimental results showed that there is no shift in mechanism within the range of operating temperature and other operating conditions. The proposed reaction mechanism is as follows:

"Oxygen not dissociated and adsorbed molecularly on dual or single sites, methane adsorbed, carbon dioxide and water adsorbed, surface reaction rate controlling."

Reproduced with permission of the copyright owner. Further reproduction prohibited without permission.

The rate equation based on the mechanism as deduced in the present investigation is only in partial agreement with the mechanistic equation arrived at by Mezaki[19].

Reproduced with permission of the copyright owner. Further reproduction prohibited without permission.

NOMENCLATURE

a, b, c	constants in initial rate equations
A, B, C	constants for linearised rate equations
ai	activity coefficient for the species i
ap	surface area per single catalyst pellet
am	surface area of pellets per unit mass
Ap	area of constriction
Cp	heat capacity at constant pressure
Cr	coefficient of discharge for a flowmeter
Cv	heat capacity at constant volume
$D_A m$	mean diffusivity of component A in a gas mixture
Dp	effective particle diameter
F	feed rate, moles per unit time
G	mass velocity lb/(hr.)(ft^2)
ΔHA	molar heat of reaction of component A
ksr	reaction velocity constant where surface reaction is rate controlling
ki	reaction velocity constant where adsorption of component i is controlling
K	overall equilibrium constant
Ki	odsorption equilibrium constant for component i
L	total number of available active sites
m, n	constants in empirical rate equation
pi	partial pressure of component i
pf	pressure factor
pc	critical pressure
pr	reduced pressure
r	rate of reaction, lb moles/(hr.)(lb. of catalyst)

Reproduced with permission of the copyright owner. Further reproduction prohibited without permission.

ro	initial rate of reaction' referred to methane
R	gas constant
Re	Reynolds number
T	absolute temperature
t	temperature, C^{o}
Tc	critical temperature, K^{o}
W	flow rate, lb./hr.
w	mass of catalyst
Xi	fraction of i converted

Greek

μ	visocity
π	total pressure, atm.
ρ	density
α', α''	constants

Reproduced with permission of the copyright owner. Further reproduction prohibited without permission.

BIBLIOGRAPHY

(1) Yocom, John E., Chemical Engineering, page 104, July 23, 1962.

(2) Faith, W.L., "Air Pollution Control", Wiley and sons Inc., N.Y., 1959.

(3) Lamb, A.B., et. al., Ind. and Eng. Chem., 12, 213 (1920).

(4) Yant, W.P. and Hawk, C.O., J. Am. Chem. Soc. 49, 1454 (1927).

(5) Cannon, W.A., and Welling, C.E., Ind. and Eng. Chem. Product Research and Development, 1, No. 3. 152 (1962).

(6) Automobile Manufacturers Association, Exhaust System Task Group, Reprint 173, August 1957.

(7) Anderson, R.B., et. al., Ind. and Eng. Chem., 53, 809 (1961).

(8) Emmet, P.H., Catalysis, Vol. VII, Reinhold Publishing Corporation, 1960.

(9) Henry, G., Phil. Mag., 65, 269 (1825).

(10) Campbell, J.R., and Thomas, G., J. Soc. Chem. Ind., 49, 432 (1930).

(11) Wheeler, T.S., Rec. Trav. Chim. 50, 874 (1931).

(12) Arneil, A., J. Soc. Chem. Ind., 53, 899 (1934).

(13) Araki, S., Japan Analyst, 2, 365 (1953).

(14) Thompson, G.P., et. al. J. Air Pollution Control Assoc., 10, 275 (1960).

(15) Kazarnovskya, L.K. and Dykhno, N.M., Kislorod 12, No. 2, 28 (1959).

(16) Cohn, J.G.E. and Haley, A.J., Can. Patent 597, 459, May 3 (1940).

(17) Rosenbaum, E.J. et. al., Anal. Chem. 31, 1006 (1959).

Reproduced with permission of the copyright owner. Further reproduction prohibited without permission.

(18) Mezaki, Reiji, "Kinetics of Catalytic Oxidation of Methane", Ph. D Thesis, University of Wisconsin, Chem. Engg. Deptt., Jan., 1963.

(19) Mezaki, Reiji and Watson Charles C., Ind. and Engg. Chem. Process Design and Development, 5, No. 1, 62 (1966).

(20) Thaller, L.H. and George Thodos, A.E. Ch. E. Journal, 6, 369 (1960).

(21) Mathur, G.P., "Initial Rate Approach to the Kinetics of Heterogenous Catalytic Reaction", Ph. D. Thesis, Northwestren University, Evanston, June1965.

(22) Hougen, O.A. and Watson K.M., "Chemical Process Principles", part III, John Wiley and Sons., N.Y., 1950.

(23) Yang K.H. and Hougen, O.A., Chem. Eng. Prog., 46, 156 (1950).

(24) Brown, G.G., et. al., "Unit Operations" John Wiley and Sons, New York, (1950).

(25) Hougen, O.A., Ind. and Eng. Chem., 53, 509 (1961).

(26) Neville Adam M. and Kennedy John B., "Basic Statistical Methods for Engineers and Scientists". International Textbook Co., Scranton (Pa.), 1964.

Reproduced with permission of the copyright owner. Further reproduction prohibited without permission.

APPENDIX I

Tables 6, 7, 8, 9, 10 and 11

Reproduced with permission of the copyright owner. Further reproduction prohibited without permission.

Table 6[6]

Composition of Auto Exhaust Gases under Different Operating Conditions - I

Operating Condition	Hydrocarbons (%)	Carbon Monoxide (%)
Idling	0.05 - 0.1	4.6
Accelrating	0.005 - 0.05	0.6
Cruising	0.02 - 0.03	1.4
Decelerating	0.4 - 1.2	2.4

Reproduced with permission of the copyright owner. Further reproduction prohibited without permission.

Table 7[6]

Composition of Auto Exhaust Gases under Different Operating Conditions - III

Constituent (Volume %, dry basis)	Operating Condition: Idling	Operating Condition: Cruise 30-50m.p.h.
Hydrocarbons C_1 and higher	0.08 - 0.15	0.02 - 0.08
Carbon Dioxide	5 - 10	3 - 14
Carbon Monoxide	3 - 10	0.2 - 5
Hydrogen	0 - 4	0 - 2
Oxygen	0 - 2	0 - 2
Nitrogen	78 - 85	78 - 85

Water vapour generally varies from 5 - 15%

Reproduced with permission of the copyright owner. Further reproduction prohibited without permission.

Table 8[6]

Composition of Auto Exhaust Gases under Different Operating Conditions - II

Constituent	Concentration p.p.m.
Methane	63 - 292
Ethane	15 - 28
Ethylene	114 - 130
Acetylene	41 - 196
Propylene and n-Butane	35 - 83
Butene	0 - 61

Car Condition 30 m.p.h.

Reproduced with permission of the copyright owner. Further reproduction prohibited without permission.

Table 9

Correlation between Space Velocity and Conversion of Methane[13]

Space Velocity ($hr.^{-1}$)	Conversion (%)
4,000	100
6,000	100
8,000	92
10,000	88
20,000	61

Reproduced with permission of the copyright owner. Further reproduction prohibited without permission.

Table 10

The Analysis of C.P. Grade Methane

Constituent	Percentage
Methane	99.05
Ethane	0.12
Carbon Dioxide	0.20
Nitrogen	0.60
Propane	0.03
Oxygen	50 p.p.m.

Reproduced with permission of the copyright owner. Further reproduction prohibited without permission.

Table 11

Operating Data for Chromatographic Analysis

Column Bath Temperature	60°C
Injector Bath Temperature	110°C
Detector Bath Temperature	110°C
Detector Filament Current	250 milliammeters
Helium Gas Flow-rate	0.25 cc. per second

Reproduced with permission of the copyright owner. Further reproduction prohibited without permission.

APPENDIX II

Calibration Curves

Reproduced with permission of the copyright owner. Further reproduction prohibited without permission.

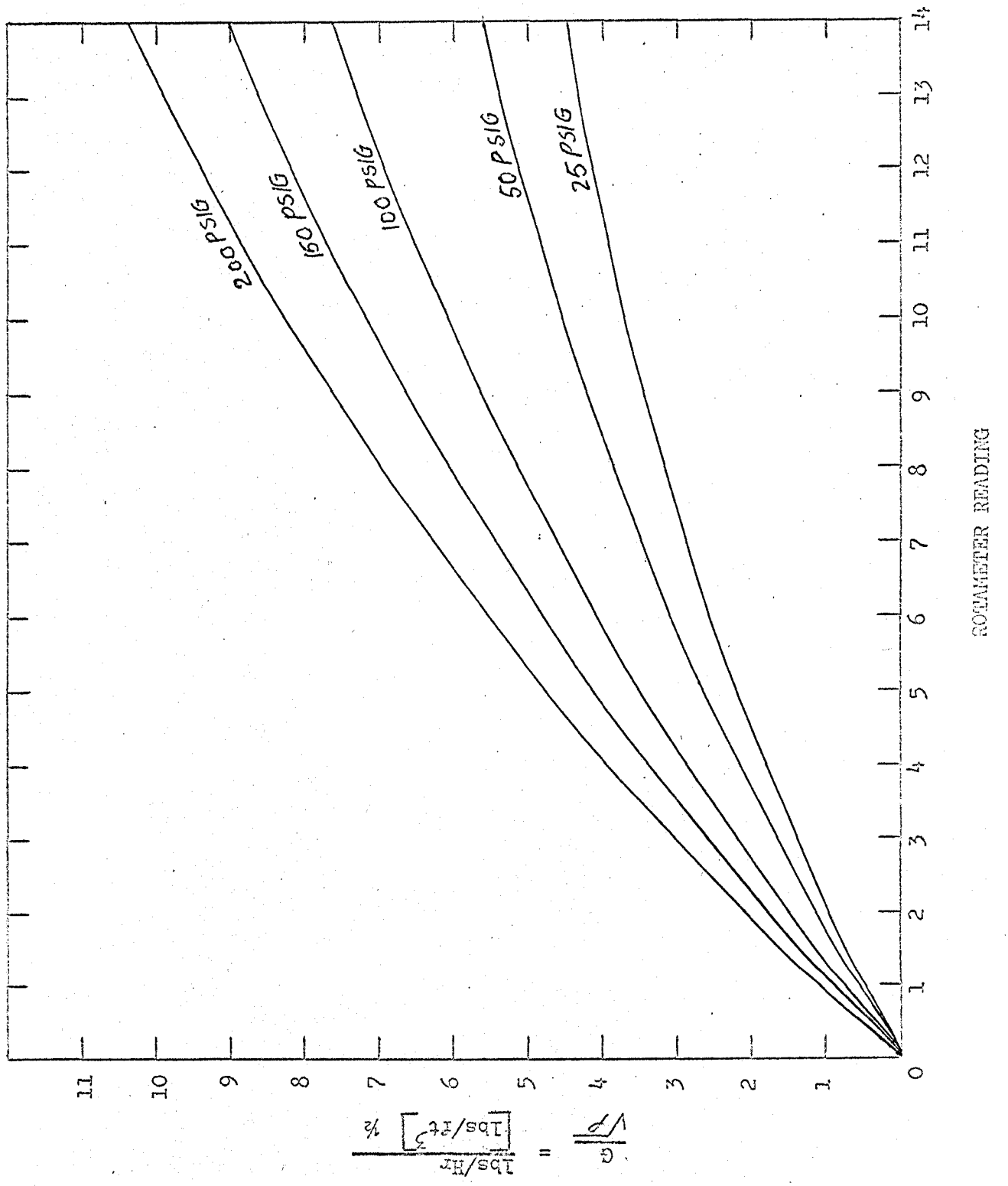

Fig. 15 CALIBRATION CURVES FOR OXYGEN ROTAMETER

Reproduced with permission of the copyright owner. Further reproduction prohibited without permission.

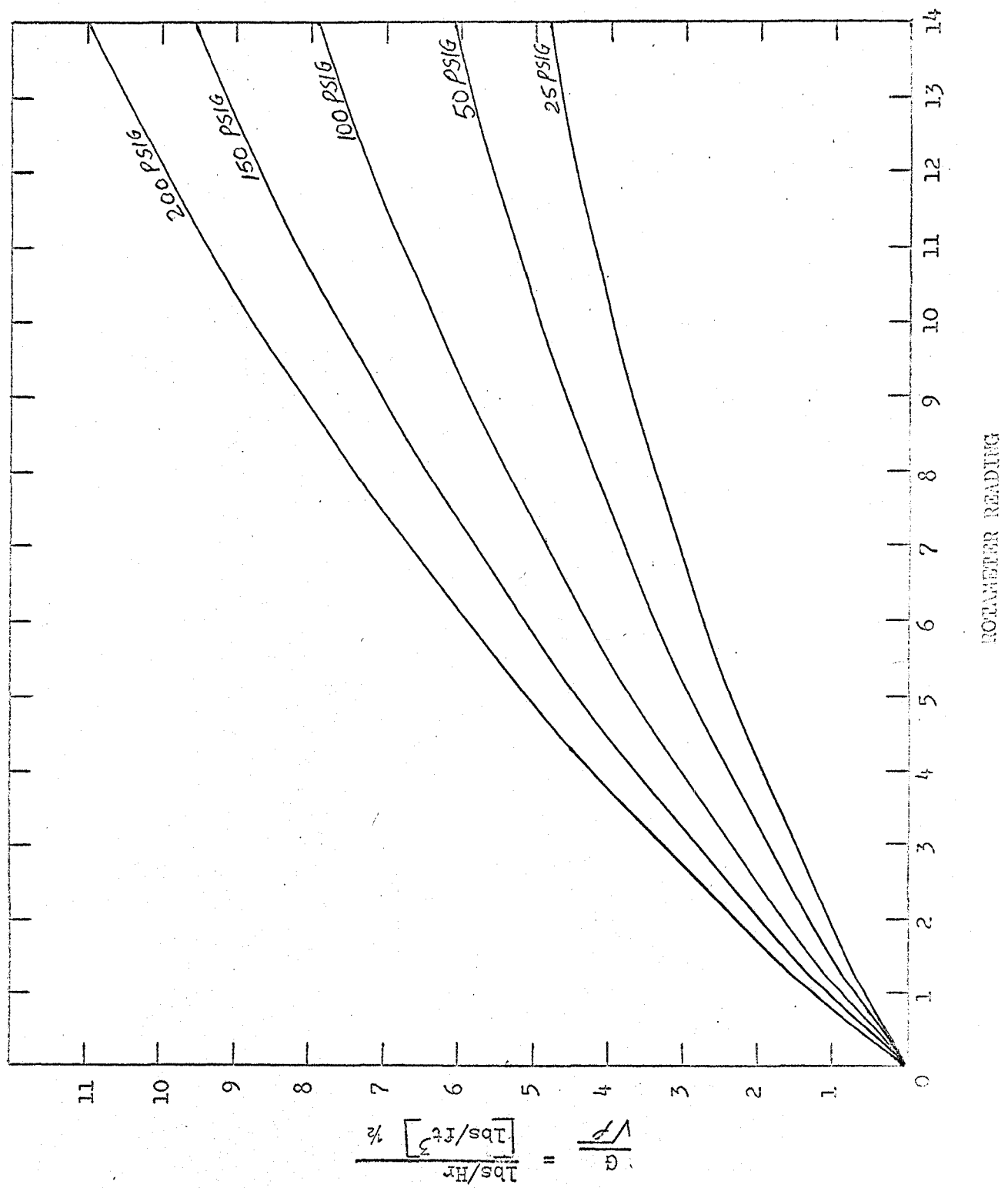

Fig. 16 CALIBRATION CURVES FOR METHANE ROTAMETER

Reproduced with permission of the copyright owner. Further reproduction prohibited without permission.

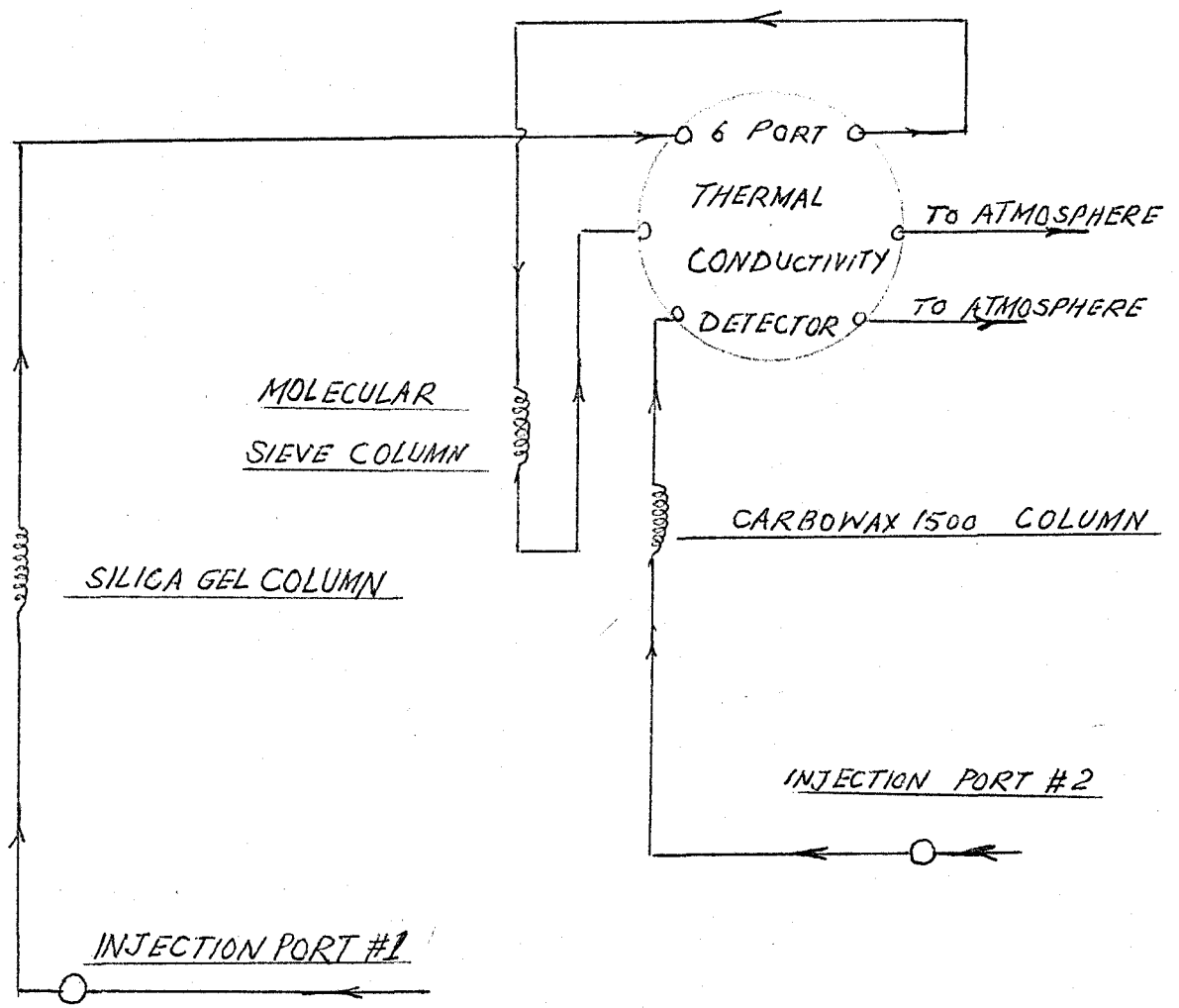

FIG. 17 ARRANGEMENT OF COLUMNS FOR 6-PORT DETECTOR

Reproduced with permission of the copyright owner. Further reproduction prohibited without permission.

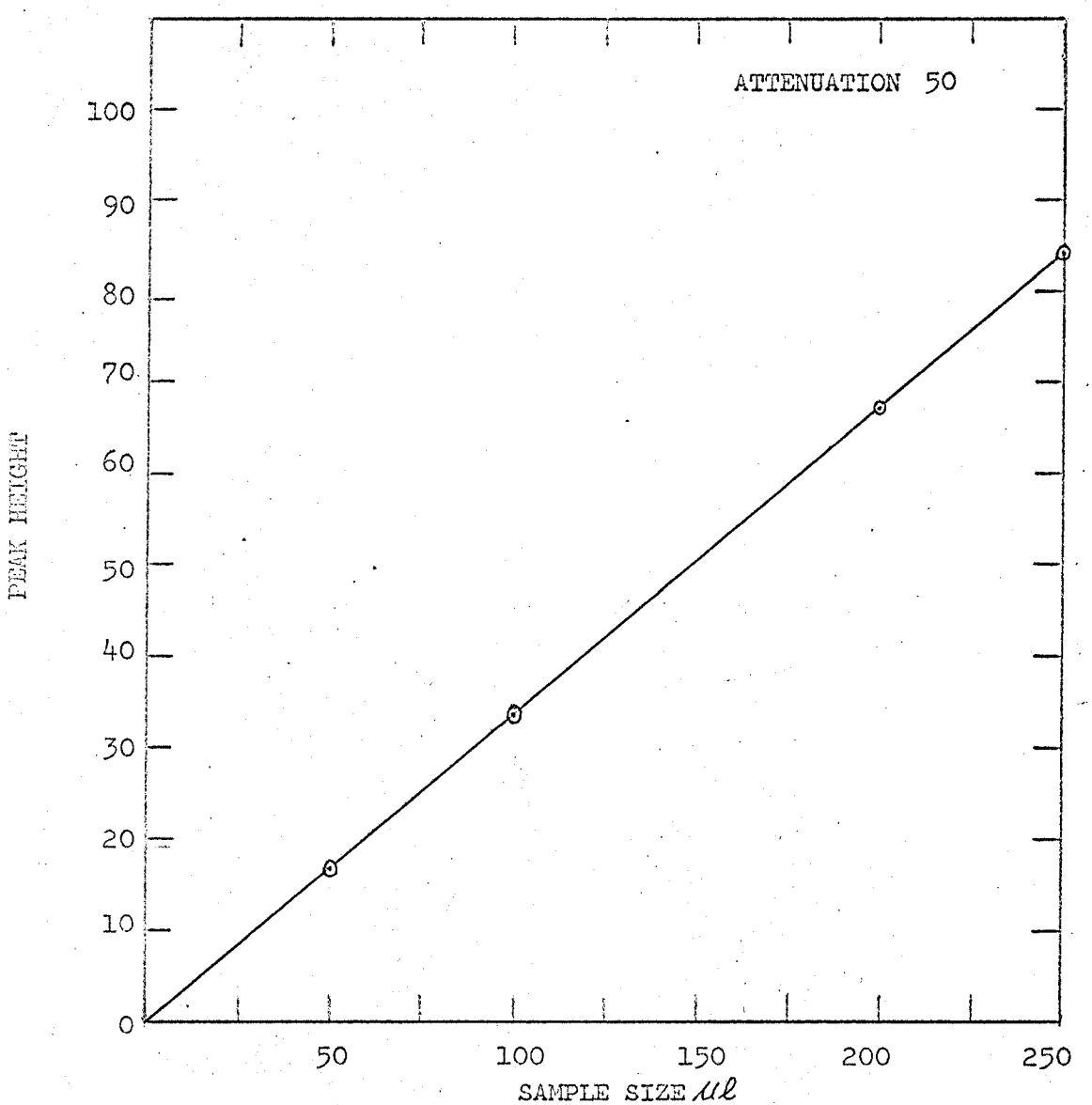

Fig. 18 CHROMATOGRAPHIC CALIBRATION FOR CARBON DIOXIDE

Reproduced with permission of the copyright owner. Further reproduction prohibited without permission.

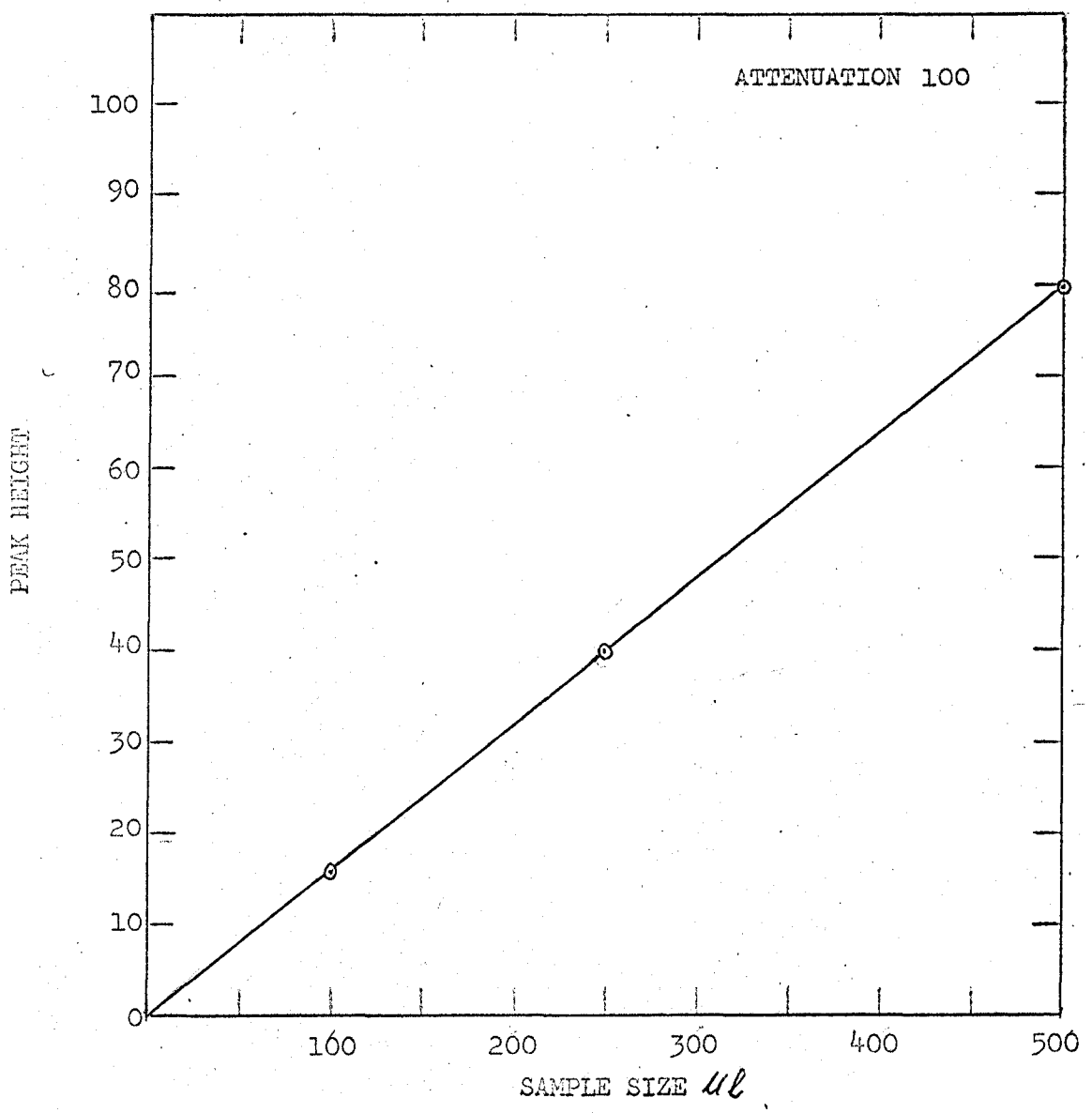

Fig. 19 CHROMATOGRAPHIC CALIBRATION FOR OXYGEN

Reproduced with permission of the copyright owner. Further reproduction prohibited without permission.

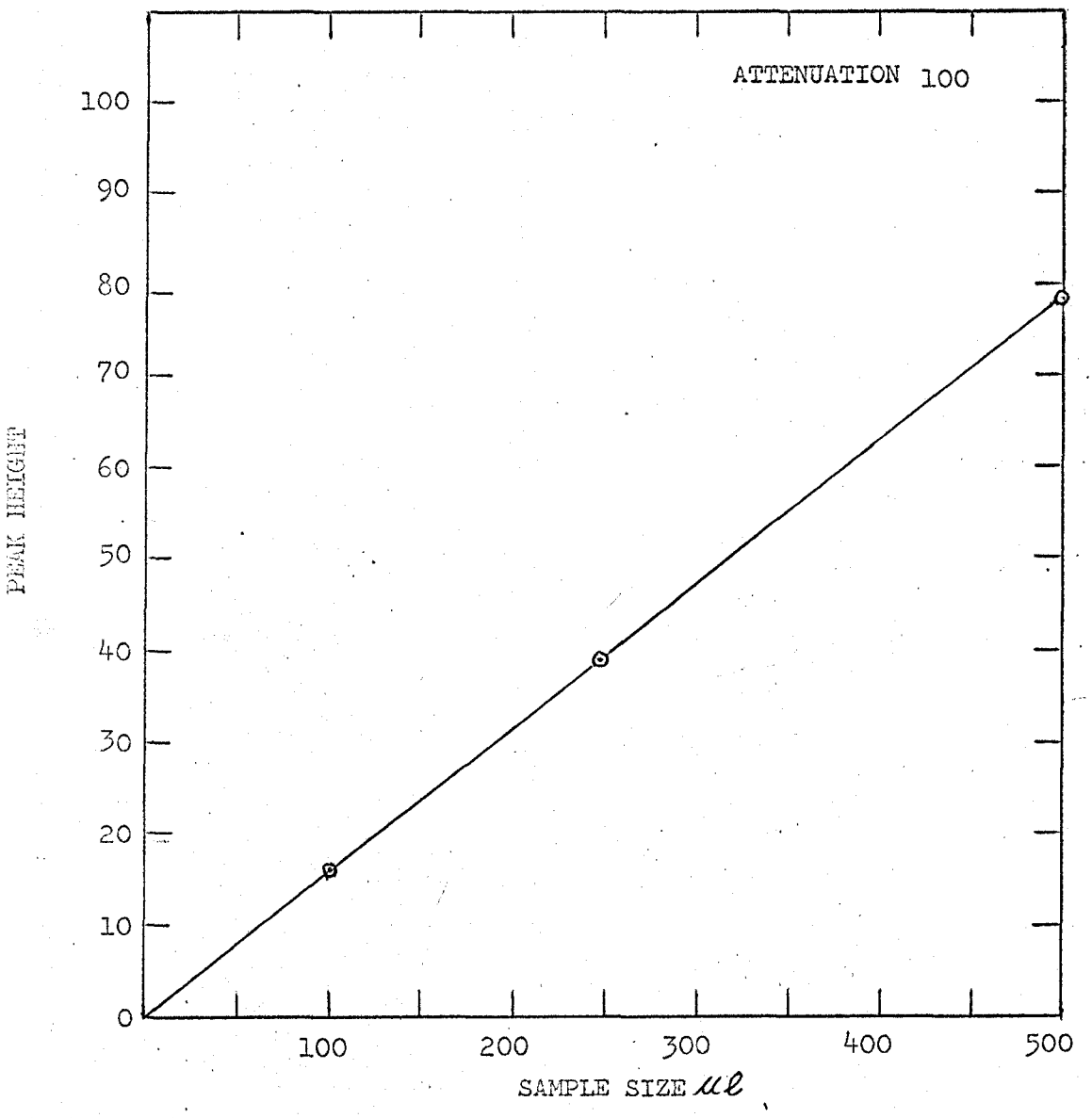

Fig. 20 CHROMATOGRAPHIC CALIBRATION FOR NITROGEN

Reproduced with permission of the copyright owner. Further reproduction prohibited without permission.

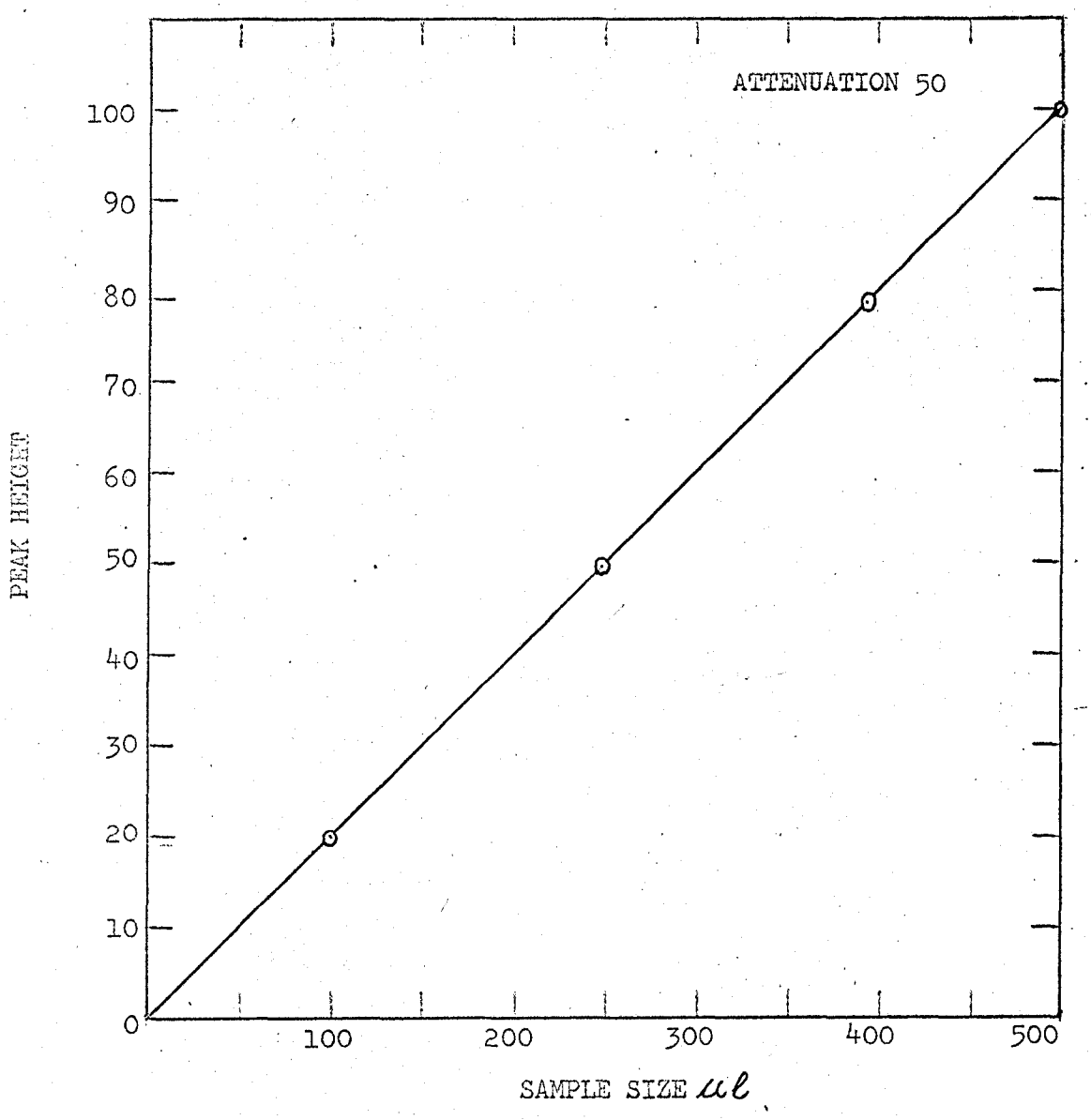

Fig. 21 CHROMATOGRAPHIC CALIBRATION FOR METHANE

Reproduced with permission of the copyright owner. Further reproduction prohibited without permission.

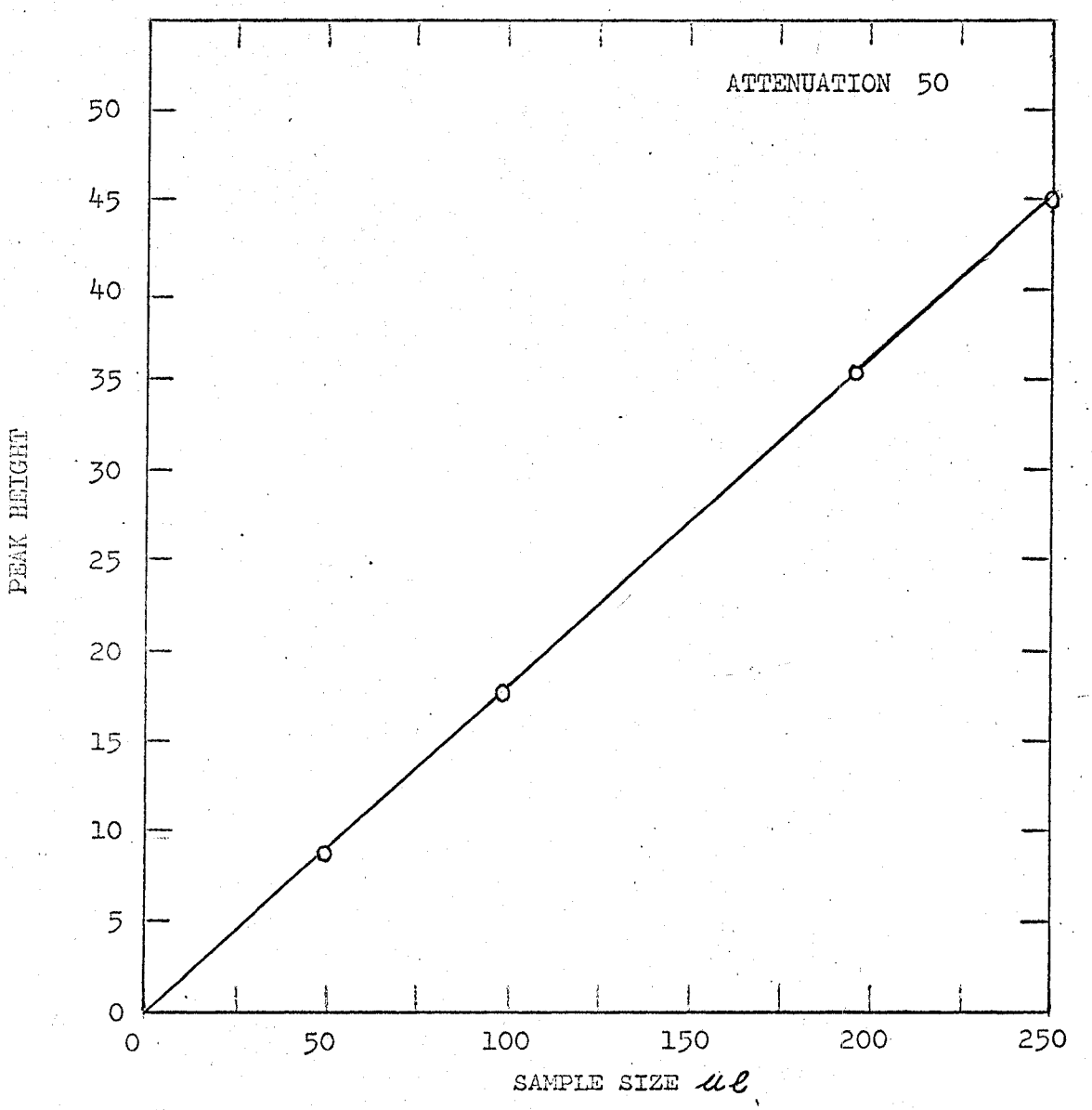

Fig. 22 CHROMATOGRAPHIC CALIBRATION FOR CARBON MONOXIDE

Reproduced with permission of the copyright owner. Further reproduction prohibited without permission.

APPENDIX III

Sample Calculation of Initial Rate from Experimental Data

UNIVERSITY OF WINDSOR LIBRARY

Reproduced with permission of the copyright owner. Further reproduction prohibited without permission.

APPENDIX III

The sample calculation is illustrated for run I-1, at 1.817 Atm. and 300°C

OXYGEN ROTAMETER

Rotameter reading = 9.0
Upstream pressure = 40 psig
Temperature = 25°C

$\frac{G}{\sqrt{P}}$ from calibration chart (fig.15) = 3.80

$G = 3.80 \times 0.552$ lbs/hr.

$= \frac{3.80 \times 0.552}{32} = 0.0664$ lb moles/hr.

weight of catalyst used = 0.498 gm.

$W = 0.498/453.6 = 1.10 \times 10^{-3}$ lb.

Product Analysis

Carbon Dioxide peak height	= 24.2	(Attenuation 2)
Oxygen peak height	= 76.1	(Attenuation 100)
Nitrogen peak height	= 0.8	(Attenuation 100)
Methane peak height	= 31.4	(Attenuation 10)

Volumes of indiviual gases in products

Carbon dioxide $= 24.2 \times \frac{250}{84 \times 25} = 2.985$ μl

Oxygen $= 76.1 \times \frac{500}{81} = 470$ μl

Nitrogen $= 0.8 \times \frac{500}{78} = 5.08$ μl

Methane $= 31.4 \times \frac{500}{100 \times 5} = 31.4$ μl

Reproduced with permission of the copyright owner. Further reproduction prohibited without permission.

Water vapour = 2 x 2.985 = 5.970 ul

Total 515.435 ul

Composition of Gases in product:

$$\text{Carbon Dioxide} = \frac{2.985}{515.435} \times 100 = 0.579\%$$

$$\text{Methane} = \frac{31.4}{515.435} \times 100 = 6.09\%$$

$$\text{Conversion} = \frac{0.579}{(0.579 + 6.09)} \times 100 = 8.66\%$$

As methane Rotameter was at very low rotameter reading, its feed rate was not calculated on rotameter reading basis, but on percentage of methane in feed gas

Methane in feed gas = 6.669%

Methane gas feed rate

$$= 0.0664 \times \frac{6.669}{93.331} = 0.474 \times 10^{-2} \text{ lb-moles/hr.}$$

Rate of reaction is given by:

$$r_0 = \frac{(\text{Feed rate of methane})\ (\%\ \text{conversion})}{(\text{Weight of catalyst}) \times 100}$$

$$= \frac{0.474 \times 10^{-2} \times 8.66}{1.1 \times 10^{-3} \times 100}$$

$$= 0.373 \quad \frac{(\text{lb moles methane})}{(\text{hr.})(\text{lb. of catalyst})}$$

Reproduced with permission of the copyright owner. Further reproduction prohibited without permission.

APPENDIX IV

Sample Calculation for Heat and Mass Transfer Effects

Reproduced with permission of the copyright owner. Further reproduction prohibited without permission.

APPENDIX IV

Yang and Hougen[22] have detailed the equations for calculating heat and mass transfer effects.

The pressure drop ΔP for any component A from the main gas stream to the gas-solid interface is given by the expression

$$\frac{\Delta p_A}{p_A} = \frac{1}{\alpha} \left(\frac{\sqrt{a_p}\, r_A\, M_m\, p_f}{p_A\, \mu\, a_m} \right) \left(\frac{\mu}{D_{Am}} \right)_F \left(\frac{\sqrt{a_p}\, G}{\mu} \right)^{n-1}$$

The equation proposed for the temperature differential across the stagnant gas film from the catalyst surface to the main gas stream is:

$$\frac{\Delta T}{T} = \frac{1}{\alpha'} \left[\frac{r_A\, \Delta HA\, \sqrt{a_p}}{a_m \cdot \mu \cdot C_p T} \right] \left[\frac{C_p\, \mu}{k} \right]_F^{2/3} \left[\frac{\sqrt{a_p}\, G}{\mu} \right]^{n-1}$$

Values of constants α, α' and n depend on Reynolds number

The result of run I-1, will be used to illustrate the method of estimating various quantities that appear in above expressions. For this run, the overall mass balance is shown below:

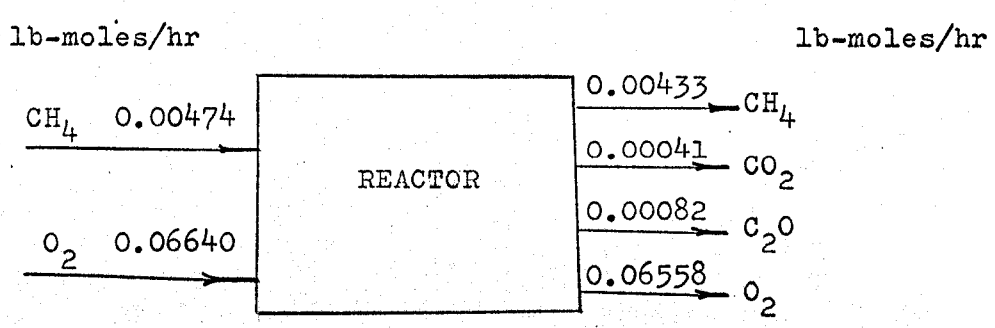

Reproduced with permission of the copyright owner. Further reproduction prohibited without permission.

Partial Pressures

Inlet

$$p_{CH_4} = \frac{0.00474}{0.0714} \times 1.817 = 0.1210 \text{ atm.}$$

$$p_{O_2} = \frac{0.0664}{0.07114} \times 1.817 = 1.6960 \text{ atm.}$$

Outlet

$$p_{CO_2} = \frac{0.00041}{0.07114} \times 1.817 = 0.01045 \text{ atm.}$$

$$p_{H_2O} = \frac{0.00082}{0.07114} \times 1.817 = 0.0209 \text{ atm.}$$

$$p_{CH_4} = \frac{0.00433}{0.07114} \times 1.817 = 0.1105 \text{ atm.}$$

$$p_{O_2} = \frac{0.06558}{0.07114} \times 1.817 = 1.6755 \text{ atm.}$$

Average

$$p_{CH_4} = 0.1157 \text{ atm.}$$

$$p_{O_2} = 1.6857 \text{ atm.}$$

$$p_{CO_2} = 0.00523 \text{ atm.}$$

$$p_{H_2O} = 0.01045 \text{ atm.}$$

Physical Properties

Critical Temperature

$$T_{cm} = \sum_i X_i \; T_{Ci}$$

$$T_{cm} = (0.0638)(190.7)+(0.9275)(154.4)+(0.00279)(304.2)+(0.00579)(647.4)$$

$$= 159.97^\circ \text{ K}$$

Reproduced with permission of the copyright owner. Further reproduction prohibited without permission.

Molecular Weight

$$Mm = \sum_i X_i \; M_i$$

$$Mm \quad (0.0638)(16)+(0.9275)(32)+(0.00279)(44)+(0.00579)(18)$$

$$= 30.7235$$

Viscosity

$$\mu_{cm} = \sum_i X_i \; \mu_{ci}$$

$$\mu_m = \mu_{cm} \; \mu_{rm}$$

$$cm \quad (0.0638)(159)+(0.9275)(250)+(0.00279)(343)+(0.00579)(495)$$

$$= 245.84 \text{ micropoise}$$

The value of μ_{rm} can be read from figure 175, page 871, Reference (21)

$$Tr = 573/159.97 \quad 3.58$$

$$Pr \cong 0$$

$$\mu_{rm} = 1.2$$

$$\mu_m = (1.2)(245.84) = 295.01 \text{ micropoise}$$

$$= 0.0956 \text{ lbs/(hr.)(ft.)}$$

Density

$$\rho_m = \frac{30.7235 \times 1.817}{0.7302 \times 1032}$$

$$= 0.0741 \text{ lbs/ft}^3$$

Diffusivity

$$(1 - X_A) \; D_{Am} = X_B \; D_{AB} + X_C \; D_{AC} + \text{----------} \; X_i \; D_{Ai}$$

$$D_{AB} = \frac{0.0043 \; T^{3/2}}{\pi \left(V_A^{1/3} + V_B^{1/3}\right)} \sqrt{\frac{1}{M_A} + \frac{1}{M_B}}$$

Reproduced with permission of the copyright owner. Further reproduction prohibited without permission.

$$D_{CH_4 - O_2} = \frac{(0.0043)(573)^{3/2}}{1.817\ (29.6^{1/3} + 25.6^{1/3})} \sqrt{\frac{1}{16} + \frac{1}{32}}$$

$$= 0.48\ cm^2/\ sec.$$
$$= 1.856\ ft^2/hr.$$

$$D_{CH_4 - CO_2} = \frac{(0.0043)(573)^{3/2}}{1.817\ (29.6^{1/3} + 34^{1/3})} \sqrt{\frac{1}{16} + \frac{1}{44}}$$

$$= 0.417\ cm^2/sec.$$
$$= 1.615\ ft^2/hr.$$

$$D_{CH_4 - H_2O} = \frac{(0.0043)(573)^{3/2}}{1.817(29.6^{1/3} + 18.9^{1/3})} \sqrt{\frac{1}{16} + \frac{1}{16}}$$

$$= 0.598\ cm^2/sec.$$
$$= 2.315\ ft^2/hr.$$

$$(1 - 0.0638)\ D_{CH_4 - m} = (1.856)(0.9275) + (1.615)(0.00279) + (2.315)(0.00579)$$

$$D_{CH_4 - m} = 1.85\ ft^2/hr.$$

<u>Pressure Film Factor</u>

$$P_f = (\pi + \delta_A\ P_A)_m$$

$$= \pi + 0 = 1.817\ atm.$$

<u>Modified Reynolds Number</u>

$$N'_{re} = \frac{\sqrt{ap.}\ G}{\mu}$$

$$G = F/A = \frac{0.00453 \times 16}{\left(\frac{\pi}{4}\right) \times \left(\frac{1.5}{12}\right)^2} = 5.91\ lbs/(hr.)(ft^2)$$

Reproduced with permission of the copyright owner. Further reproduction prohibited without permission.

$$D_p = (1.5)^{1/2} D = (1.5)^{1/2}\left(\frac{1}{8 \times 12}\right) = 0.0127 \text{ ft.}$$

$$a_p = \pi D_p^2 = 0.000507 \text{ ft}^2$$

Modified Reynolds Number

$$N'_{Re} = \frac{(a_p)^{1/2} G}{\mu} = \frac{(0.000507)^{1/2} (5.91)}{0.0956}$$

$$= 1.391$$

Schmidt Number

$$S_c = \frac{\mu}{P D_{Am}} = \frac{0.0956}{(7.41 \times 10^{-2})(1.85)} = 0.698$$

$$A_m = 120 \text{ (metre)}^2/\text{gm} \qquad \text{(Suppliers Data)}$$

$$= \frac{120 \times (3.28)^2}{1/453.6} = 5.8 \times 10^5 \text{ (ft)}^2/\text{ lb.}$$

Pressure Drop

The pressure drop for methane from the main gas stream to the gas-solid interface is given as

$$\frac{\Delta p_A}{p_A} = \frac{1}{\alpha}\left[\frac{\sqrt{a_p}\, r_A\, M_m\, p_f}{p_A\, \mu\, a_m}\right]\left[\frac{\mu}{P\, D_{Am}}\right]_f \left[\frac{\sqrt{a_p} G}{\mu}\right]^{n-1}$$

for $N'_{re} < 620$, $\alpha = 2.44$ and $n = 0.51$

$$\therefore \frac{\Delta p}{p} = \frac{1}{2.44}\left[\frac{(0.000507)^{1/2}(0.373)(30.7235)(1.817)}{(0.1157)(0.0956)(5.8 \times 10^5)}\right](0.698)^{2/3}(1.391)^{1-0.5}$$

Reproduced with permission of the copyright owner. Further reproduction prohibited without permission.

$$\frac{\Delta p}{p} = 2.01 \times 10^{-3}$$

$$\Delta P = 2.01 \times 10^{-3} \times 0.1157 = 2.33 \times 10^{-4} \text{ atm.}$$

Specific Heat

$$C_{pm} = \sum_i X_i C_{p_i}$$

$$= (0.0638)(12.32)+(0.9275)(7.68)+(0.00279)(11.2)+(0.00579)(3.96)$$

$$= 7.957 \quad \text{Btu/(lb-mole)(R}^{\circ}\text{)}$$

$$= 7.957 \quad \text{Cal/(gm-mole)(K}^{\circ}\text{)}$$

Prandtl Number

$$Pr = \frac{C_p \mu}{k}$$

A relation recommended by Hougen and Watson [21], is given on page 990, equation (51).

$$\frac{C_p \mu}{k} = \frac{4}{\left[9 - 5 \frac{Cv}{Cp}\right]}$$

$$\left[\frac{C_p \mu}{k}\right]^{2/3} = \left[\frac{4}{9 - \left(5 \times \frac{1}{13.1}\right)}\right]^{2/3} = 0.844$$

Heat of Reaction

$$\Delta Hr = -191 \quad \text{K. Cal/g-mole at } 500^{\circ}\text{K}$$

Reproduced with permission of the copyright owner. Further reproduction prohibited without permission.

Temperature Drop

The temperature differential ΔT across the stagnant gas film from the catalyst surface to the main gas stream is

$$\frac{\Delta T}{T} = \frac{1}{\alpha'} \left[\frac{r_A \quad \Delta H_A \quad (a_p)^{1/2}}{a_m \qquad C_p T} \right] \left[\frac{C_p \mu}{k} \right]_f^{2/3} \left[\frac{(a_p)^{1/2} \quad G}{\mu} \right]^{n-1}$$

For $N'_{re} < 620$ $\qquad \alpha' = 2.62 \qquad n = 0.51$

$$\therefore \quad \frac{\Delta T}{T} = \frac{1}{2.62} \left[\frac{0.373 \times 1.91 \times 10^5 \times 2.255 \times 10^{-2}}{5.8 \times 10^5 \times 0.0956 \times \left(\frac{7.957}{30.7235}\right) \times 573} \right] (0.844)(1.391)^{1-0.51}$$

$$= 1.345 \times 10^{-4}$$

$$\Delta T = 1.345 \times 10^{-4} \times 573 = 0.077^{\circ}C$$

It is evident, that mass transfer and heat transfer effects are quite negligible. For other runs, the mass and heat transfer contributions were found to be of the same order of magnitude as this particular run.

Reproduced with permission of the copyright owner. Further reproduction prohibited without permission.

APPENDIX V

Computer Programmes and Results

Reproduced with permission of the copyright owner. Further reproduction prohibited without permission.

```
C   C   O. P. AHUJA
C       REGRESSION  COEFFICIENTS  FOR  THE  MECHANISM   EQUATIONS  NO. 1
        DIMENSION X(10),        SIGY(10),SIGYY(10),XY(10),A(10),B(10),P(10
       1R(10),Y(10,10)
      1 READ 2, (P(K),K=1,8),(R(K),K=1,8)
        C = 8
        F = 1./3.
        DO 3 K = 1,8
        X(K) = P(K)
        Y(1,K) = P(K)/SQRTF(R(K))
        Y(2,K) =  P(K)/R(K)**F
        Y(3,K) = (P(K)**1.5)/SQRTF(R(K))
        Y(4,K) = (P(K)**3.)/R(K)
        Y(5,K) = P(K)/R(K)
        Y(6,K) = (SQRTF(P(K)))/R(K)**.25
        Y(7,K) = (P(K)**.75)/R(K)**.25
      3 Y(8,K) = P(K)/R(K)
        SIGX = 0
        SIGXX = 0
        DO 4 J = 1,8
        SIGY(J) = 0
      4 XY(J) = 0
        DO 5 J = 1,8
        DO 5 K = 1,8
        SIGY(J) = SIGY(J) + Y(J,K)
      5 XY(J) = XY(J) + X(K) * Y(J,K)
        DO 6 K = 1,8
        SIGX = SIGX + X(K)
      6 SIGXX = SIGXX + X(K)*X(K)
        DO 7 J = 1,8
        A(J) = (SIGXX*SIGY(J)-SIGX*XY(J))/(C*SIGXX-SIGX*SIGX)
      7 B(J) = (C*XY(J)-SIGX*SIGY(J))/(C*SIGXX-SIGX*SIGX)
        PUNCH 10
        DO 9 J = 1,8
      9 PUNCH 8,J,A(J),B(J)
      2 FORMAT(8F8.3/(8F8.3))
     10 FORMAT(5X,1HN,15X,1HA,20X,1HB//)
      8 FORMAT(5X,I1, 2(10X,F12.6))
        GO TO 1
        END
      1817    2975    3925    5220    6240    7130    8410    97
       373     481     503     559     594     624     655     671
      1817    2975    3925    5220    6240    7130    8410    97
       398     511     531     581     616     658     694     712
      1817    2975    3925    5220    6240    7130    8410    97
       421     552     580     640     673     720     745     771
```

Reproduced with permission of the copyright owner. Further reproduction prohibited without permission.

O. P. AHUJA

REGRESSION COEFFICIENTS FOR THE MECHANISM EQUATIONS NO. 1

TEMPRATURE 300 DEGREES C

N	A	B
1	1.034149	1.119909
2	.622627	1.082035
3	-4.980518	4.172677
4	-471.924620	164.676080
5	2.818439	1.208295
6	1.448114	.214024
7	1.218984	.511810
8	2.818439	1.208295

TEMPRATURE 320 DEGREES C

N	A	B
1	1.018676	1.088979
2	.619577	1.061949
3	-4.797862	4.055110
4	-443.534080	155.399770
5	2.692498	1.143425
6	1.429209	.211230
7	1.205102	.504798
8	2.692498	1.143425

TEMPRATURE 340 DEGREES C

N	A	B
1	.973950	1.045676
2	.599482	1.033754
3	-4.642242	3.898043
4	-411.557960	143.724510
5	2.484799	1.052355
6	1.402137	.206615
7	1.180958	.494457
8	2.484799	1.052355

Reproduced with permission of the copyright owner. Further reproduction prohibited without permission.

```
C       O. P. AHUJA
C       REGRESSION  COEFFICIENTS  FOR  MECHANISM  EQUATION  NO.  9
        DIMENSIONX(15),Y(15),Z(15),P(15),R(15)
      6 READ 5, (P(K),K=1,8),(R(K),K=1,8)
        DO 1 J=1,8
        X(J) = P(J)
        Y(J) = SQRTF(P(J))
      1 Z(J) = (P(J)**0.6)/(R(J)**.2)
        SIGX = 0
        SIGY = 0
        SIGZ = 0
        SIGXX = 0
        SIGYY = 0
        SIGXY = 0
        SIGYZ = 0
        SIGZX = 0
        DO 2 J = 1,8
        SIGX = SIGX + X(J)
        SIGY = SIGY + Y(J)
        SIGZ = SIGZ + Z(J)
        SIGXX = SIGXX + X(J)*X(J)
        SIGYY = SIGYY + Y(J)*Y(J)
        SIGXY = SIGXY + X(J)*Y(J)
        SIGYZ = SIGYZ + Y(J)*Z(J)
      2 SIGZX = SIGZX + Z(J)*X(J)
        PUNCH 3,SIGZ,SIGX,SIGY
        PUNCH 4,SIGZX,SIGX,SIGXX,SIGXY
        PUNCH 4,SIGYZ,SIGY,SIGXY,SIGYY
      3 FORMAT(F9.4,2H =,6H  8 B0,3H + ,2HB1,F9.4,2H +,3H B2,F9.4//)
      4 FORMAT(F9.4,5H    =,3H B0,F9.4,2H +,3H B1,F9.4,3H + ,2HB2,F9.4//)
      5 FORMAT(8F8.3/(8F8.3))
        GO TO 6
        END
     1817    2975    3925    5220    6240    7130    8410    97
      373     481     503     559     594     624     655     671
     1817    2975    3925    5220    6240    7130    8410    97
      398     511     531     581     616     658     694     712
     1817    2975    3925    5220    6240    7130    8410    97
      421     552     580     640     673     720     745     771
```

Reproduced with permission of the copyright owner. Further reproduction prohibited without permission.

O. P. AHUJA

REGRESSION COEFFICIENTS FOR MECHANISM EQUATION NO. 9

TEMPRATURE = 300 DEGREES C

24.6427 = 8 B0 + B1 45.4170 + B2 18.5213

155.9711 = B0 45.4170 + B1 309.3987 + B2 116.5084

60.6336 = B0 18.5213 + B1 116.5084 + B2 45.4169

TEMPRATURE = 320 DEGREES C

24.3854 = 8 B0 + B1 45.4170 + B2 18.5213

154.3376 = B0 45.4170 + B1 309.3987 + B2 116.5084

60.0016 = B0 18.5213 + B1 116.5084 + B2 45.4169

TEMPRATURE = 340 DEGREES C

23.9883 = 8 B0 + B1 45.4170 + B2 18.5213

151.8152 = B0 45.4170 + B1 309.3987 + B2 116.5084

59.0200 = B0 18.5213 + B1 116.5084 + B2 45.4169

Reproduced with permission of the copyright owner. Further reproduction prohibited without permission.

```
C       O. P. AHUJA                                                    95
C       COEFFICIENTS  FOR  THE  EMPIRICAL  RATE  EQUATION
        DIMENSION X(15),Y(15),Z(15),A(15),B(15),R(15)
      6 READ 5,(A(J),J=1,10),(B(J),J=1,10),(R(J),J=1,10)
        DO 1 J=1,10
        X(J) = LOGF(A(J))
        Y(J) = LOGF(B(J))
      1 Z(J) = LOGF(R(J))
        SIGX = 0
        SIGY = 0
        SIGZ = 0
        SIGXX = 0
        SIGYY = 0
        SIGXY = 0
        SIGYZ = 0
        SIGZX = 0
        DO 2 J = 1,10
        SIGX = SIGX + X(J)
        SIGY = SIGY + Y(J)
        SIGZ = SIGZ + Z(J)
        SIGXX = SIGXX + X(J)*X(J)
        SIGYY = SIGYY + Y(J)*Y(J)
        SIGXY = SIGXY + X(J)*Y(J)
        SIGYZ = SIGYZ + Y(J)*Z(J)
      2 SIGZX = SIGZX + Z(J)*X(J)
        PUNCH 3,SIGZ,SIGX,SIGY
        PUNCH 4,SIGZX,SIGX,SIGXX,SIGXY
        PUNCH 4,SIGYZ,SIGY,SIGXY,SIGYY
      3 FORMAT(F9.4,2H =,6H 10 B0,3H + ,2HB1,F9.4,2H +,3H B2,F9.4//)
      4 FORMAT(F9.4,5H     =,3H B0,F9.4,2H +,3H B1,F9.4,3H + ,2HB2,F9.4//)
      5 FORMAT(10F6.6/(10F6.4)/(10F6.3))
        GO TO 6
        END
 4740  6280  7125  8160  8800  9610 11171 12310 11793 251
  664   906  1029  1173  1270  1392  1610  1753   664   664
  373   481   503   559   594   624   655   671   796   842
 481   632   724   812   877   958  1123  1225  1177  2497
  664   906  1029  1173  1270  1392  1610  1753   664   664
  398   511   531   581   616   658   694   712   836   884
 484   639   72    819   886   971   112  1232  1175  2531
  664   906  1029  1173  1270  1392  1610  1753   664   664
  421   552   580   640   673   720   745   771   882   932
```

Reproduced with permission of the copyright owner. Further reproduction prohibited without permission.

O. P. AHUJA

COEFFICIENTS FOR THE EMPIRICAL RATE EQUATION

TEMPRATURE = 300 DEGREES C

-5.2015 = 10 B0 + B1 -46.5696 + B2 -22.5575

25.1416 = B0 -46.5696 + B1 218.7236 + B2 105.0645

11.7985 = B0 -22.5575 + B1 105.0645 + B2 52.1096

TEMPRATURE = 320 DEGREE C

-4.6791 = 10 B0 + B1 -46.5508 + B2 -22.5575

22.6762 = B0 -46.5508 + B1 218.5045 + B2 105.0151

10.6178 = B0 -22.5575 + B1 105.0151 + B2 52.1096

TEMPRATURE = 340 DEGREES C

-3.9252 = 10 B0 + B1 -46.4920 + B2 -22.5575

19.1228 = B0 -46.4920 + B1 217.9665 + B2 104.8812

8.9551 = B0 -22.5575 + B1 104.8812 + B2 52.1096

Reproduced with permission of the copyright owner. Further reproduction prohibited without permission.

VITA AUCTORIS

1937	Born Om Parkash Ahuja on June 8, 1937, in Bhera, Surgodha. India.
1953	Completed science matriculation at Arya High School, Panipat, India.
1957	Graduated in science, D.S. College, Karnal, India.
1961	Graduated in Chemical Engineering, Indian Institute of Technology, Kharagpur, India.
1961-64	Employed in Design and Development section of DCM Chemical Works, New Delhi, India.
1964	Accepted into the Graduate School of University of Windsor as Candidate for the degree of M. A. Sc. in Chemical Engineering.
1966	Working as project Engineer, Canadian Celanese, Drummondville (Quebec).

Reproduced with permission of the copyright owner. Further reproduction prohibited without permission.